Survey of Earth-Mars Trajectories using Lambert's Problem and Applications

Thesis · December 2013

DOI: 10.13140/RG.2.2.11589.55525

1 author:

Davide Conte
Pennsylvania State University
24 PUBLICATIONS **20** CITATIONS

SEE PROFILE

THE PENNSYLVANIA STATE UNIVERSITY
SCHREYER HONORS COLLEGE

DEPARTMENT OF AEROSPACE ENGINEERING

SURVEY OF EARTH-MARS TRAJECTORIES USING LAMBERT'S PROBLEM AND APPLICATIONS

DAVIDE CONTE
Spring 2014

A thesis
submitted in partial fulfillment
of the requirements
for baccalaureate degrees
in Aerospace Engineering and Mathematics
with honors in Aerospace Engineering

Reviewed and approved* by the following:

David B. Spencer
Professor of Aerospace Engineering
Thesis Supervisor

Robert G. Melton
Professor of Aerospace Engineering
Director of Undergraduate Studies

George A. Lesieutre
Professor of Aerospace Engineering
Head of the Department of Aerospace Engineering
Honors Adviser

* Signatures are on file in the Schreyer Honors College.

ABSTRACT

The focus of this thesis is to analyze interplanetary transfer maneuvers from Earth to Mars by solving Lambert's Problem. Additionally, the orbital parameters of the transfer orbits as well as the relative required ΔVs and times of flights were determined in order to define the optimal departure and arrival windows for a given range of date. The first step in solving Lambert's Problem consists in finding the positions and velocities of the departure (Earth) and arrival (Mars) planets for a given range of dates. Then, by solving Lambert's problem for various combinations of departure and arrival dates, porkchop plots can be created and examined. Some of the key parameters that are plotted on porkchop plots and used to investigate possible transfer orbits are the departure characteristic energy, C3, and the arrival v_∞. These parameters, in combination with given desired initial and final parking orbital conditions about Earth and Mars, were also used to determine the total ΔV for the various Earth-Mars transfers. Lastly, ΔV results were used to find the necessary amount of propellant needed for the transfer maneuvers as a percentage of total spacecraft mass for a given specific impulse.

Moreover, this thesis also considers cases when Lambert's solution fails to give reasonable results, particularly when the transfer angle between Earth and Mars is close to 0 or 180 degrees. A special case of Lambert's problem is the Hohmann transfer, which is also discussed in this thesis.

The results of the analysis lead to the choice of departure and arrival dates that, given the capabilities of the launch system such as ΔV, makes the mission feasible. Additionally, unless specified otherwise, only time of flight that would be reasonable for an unmanned mission to Mars were considered.

TABLE OF CONTENTS

LIST OF FIGURES

LIST OF TABLES

ACKNOWLEDGEMENTS

I would like to thank Dr. Spencer for all of the help he gave me in writing this thesis, and especially for teaching Interplanetary Astrodynamics, one of the most exciting classes I have taken at Penn State.

I would also like to acknowledge Dr. Melton and Dr. Lesieutre for the teachings and advices they have given me throughout my college career.

Additionally, I would like to thank Dr. Parsons who has given me the mathematical foundations and the support to succeed in my later years at Penn State.

Since I was a child, my dad would take me outside on our balcony and show me the splendors of the universe through the lenses of our telescope. Soon, the love for space my family had given me combined with the passion for science, mathematics, and engineering made me realize that I wanted to make a difference in the future of space exploration. Everything I have worked on, especially during the past five years, was made possible by my parents, Giovanni and Rossana, and my sister, Lucia. Their love and financial support have given me the opportunity to study thousands of miles away from home in one of the best universities in the world. And while I occasionally doubted my own abilities, they never did. Lucia, mamma e papà, grazie di cuore per tutto ciò che avete fatto per me, per gli aiuti morali ed economici che mi avete dato, per i consigli che ho ricevuto nei momenti difficili e per la gioia che mi date quando ci sentiamo e vediamo su internet e soprattutto per la gioia che mi date quando torno a casa in Italia. Anche se forse vi verrà difficile capire alcune delle sue parti, vi dedico questa tesi.

I also would like to thank Sour Roberta, my elementary school teacher, who has supported me with her prayers and thoughts.

A special thanks goes to the many friends I have made in America since I started studying abroad. Dedico questa tesi anche ai miei amici italiani. Grazie per il vostro supporto e per la vostra ineguagliabile amicizia.

Finally, I would like to thank all of the engineers, scientists, and technicians who work towards space exploration and towards answering the fundamental questions of our seemingly infinite Universe. Their work is an inspiration for me and gives me hope that seeing humans walk on the surface of Mars and other celestial bodies will soon become a reality.

Chapter 1

Introduction

Humanity has always had the desire to explore. In fact, exploration is indeed found within the innate sense of curiosity and enthusiasm that mankind possesses. From religious meaning, depicted as the angry god of war, to astronomical interest because of its strange and apparent retrograde motion, Mars, also known as the red planet, is still considered a remote destination, yet to be reached by humans. In order to fully understand and answer some of the fundamental questions about the formation of our Solar System and the development of life on our planet, interplanetary space exploration has gradually become a necessity.

Due to the recent budget cuts, space mission cost has become a more important key factor in deciding whether a mission will take place. In fact, the cost of unmanned space missions to Mars ranges from a few hundreds millions to billions of USD. For example, the Mars Science Laboratory (MSL) was $2.5 billion USD.[8] Additionally, traditional chemical propulsion systems having a specific impulse (Isp) of 300-350 seconds require 80-85% of the total spacecraft mass to be propellant, allowing only for relatively small payloads to be delivered to Mars. Therefore, it is clear that it is necessary to make propellant-efficient decisions starting from the orbital trajectory design. Optimal trajectories will not only reduce the cost of missions to Mars, but they will also allow for more massive payloads to be transported in orbit around and possibly land on the red planet.

This thesis presents a method of determining the interplanetary transfer orbit parameters, the required ΔVs to achieve the Earth-Mars trajectory, and the payload to propellant mass ratio

for given user defined conditions including: departure and arrival dates, Earth and Mars parking orbits altitudes, and specific impulse.

Assumptions

The assumptions that were used throughout the analysis of the transfer maneuvers are as follows:

1. All the ΔV maneuvers are treated as impulsive; assuming the use of chemical or nuclear propulsion systems, the burn times required for such ΔVs (in the order of minutes or hours) are considerably much less than the orbital transfer times from Earth to Mars (in the order of months).

2. The only major forces that were considered for the analysis are the point mass gravitational forces of Earth, Mars and the Sun within their respective spheres of influence. Perturbations such as solar radiation pressure, non-uniform gravitational fields, and gravitational effects of other bodies, such as the other planets of the Solar System, were neglected.

3. The method of patched conics was used. This method assumes that when a spacecraft is outside the sphere of influence of a planet, it follows an unperturbed Keplerian orbit (i.e. two-body dynamics) around the Sun. Since interplanetary distances are so vast, for heliocentric orbits it is reasonable to neglect the size of the spheres of influence of Earth and Mars, and consider them to be just points in space coinciding with the planetary centers. Additionally, within each planet's sphere of influence, the spacecraft travels an unperturbed Keplerian path about the planet. While the sphere of influence appears small on the scale of the solar system, from the point of view of the planet it is "large enough" to be considered to extend to infinity.

MATLAB

MATLAB® is a high-level language and interactive environment for numerical computation, visualization, and programming. [4] MATLAB was used in this research to implement the necessary algorithms into computer codes as shown in the flowcharts of Appendix A and Appendix B. All the graphical results shown in this thesis were obtained by running the appropriate MATLAB scripts.

Lambert's Problem

Most of the analysis conducted in this thesis is based on the formulation and solution of a problem in the field of astrodynamics that the Swiss mathematician Johann Heinrich Lambert (1728 – 1779) formulated in 1761[10]. This problem is now known as Lambert's problem. In spacecraft targeting applications, it is essential to know the time of flight required to travel a particular trajectory. In fact, as discussed in greater details in Chapter3, Lambert's problem is a boundary value problem involving two position vectors and a time of flight between them. Additionally, according to Lambert's conjecture, only these three parameters, two position vectors and time of flight, are necessary to uniquely define an orbital transfer between the two points. From the solution to Lambert's problem it is then possible to calculate the required ΔVs.

In the case of an Earth-Mars transfer, the first step required to set up Lambert's problem is being able to identify Earth's and Mars' positions for given departure and arrival dates. Chapter 2 discusses how to obtain the position and velocity vectors of the two planets as a function of time.

Chapter 2

Determining Position and Velocity Vectors of Earth and Mars for a Given Date

In order to analyze possible transfer orbits from Earth to Mars it is necessary to obtain the position and velocity vectors of the planets at the desired departure and arrival dates. Various method to do so exist, but in this thesis only two main methods are considered: Standish's algorithm[12] and JPL HORIZONS[14]. Note that the orbital position and velocity of Earth and Mars are described by three-dimensional vectors although the transfer orbit between the two planets is a two-dimensional transfer. In fact, the orbital transfer defines a plane on which the Sun, the Earth at departure and Mars at arrival lie on.

Position Vectors of Earth and Mars

Determining the position and velocity vectors of Earth and Mars can be done using the results presented in Standish. Here, a detailed algorithm of how to determine the position of the eight planets (Mercury through Neptune) and Pluto for a given date is offered. Note that such dates must be inputted as Julian Ephemeris Dates. To convert dates from the everyday day/month/year format to Julian Dates, Algorithm 14 taken from Vallado, p.189[13]. Additionally, it must be noted that Standish's algorithm provides approximate positions for the planets. This method should not be used unless its errors are acceptable for the application taken into account. High precision ephemerides for the planets are available via the JPL HORIZONS system. The analysis and the following results presented in this thesis are based on the accuracy of Standish's algorithm, although a comparison with the HORIZONS system was also done.

Once the position vectors of Earth and Mars are obtained, it is important to make sure that both vectors are expressed in the same inertial reference frame. For simplicity and convenience, the J2000 ecliptic plane was used. By definition, this plane contains both the Sun and Earth. Additionally, this reference frame is defined by having the x-axis aligned with Earth's vernal equinox, the z-axis pointing normal to the ecliptic plane, while the y-axis completes the right-handed coordinate system as shown in Figure 1. Moreover, the z-position of Earth with respect to the Sun is exactly zero on January 1, 2000. Standish's algorithm makes use of the J2000 ecliptic plane as described above. The reference frame in which HORIZONS works can be chosen from a set of predefined reference frames, and it was set to the J2000 ecliptic reference frame for the following applications.

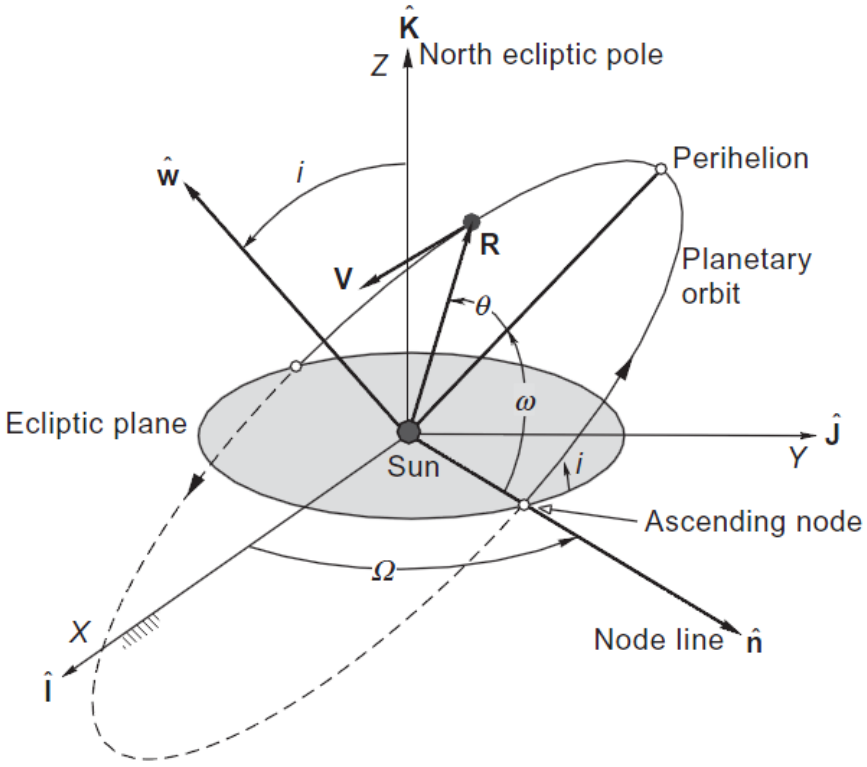

Figure 1 – Planetary orbit in heliocentric ecliptic frame; in the figure, R and V are respectively the position and the velocity vectors of the planet taken into consideration. Source: Curtis, p.471.[7]

For example, consider an arbitrary date, say January 22, 2014 at 00:00:00.0 (UT). The position vectors of Earth and Mars in J2000 ecliptic reference frame are given as shown in Table 1. Comparing the results obtained by using Standish's algorithm with those of JPL HORIZONS, it can be noted that the difference is relatively small. In fact, for the purpose of the analysis done in this thesis, the results obtained using Standish's algorithm are sufficient. Additionally, note that the position vector of a planet can be expressed as:

$$\vec{r}^{E} = r_x\hat{I} + r_y\hat{J} + r_z\hat{K} \tag{1}$$

where $\hat{I}, \hat{J}, \hat{K}$ are the unit vectors that define the J2000 ecliptic coordinate frame, 'E'.

Table 1 – Comparison between position vectors of Earth and Mars using Standish's algorithm and using JPL HORIZONS; note that the z-component is considerably smaller than the x and y components.

Earth's Position (AU) on January 22, 2014 at 00:00:00.0 (UT)			
	r_x	r_y	r_z
Standish's algorithm	-0.51686	0.83751	-0.000026827
JPL HORIZONS	-0.51570	0.83531	-0.000120055
Mars' Position (AU) on January 22, 2014 at 00:00:00.0 (UT)			
	r_x	r_y	r_z
Standish's algorithm	-1.60258	0.44615	0.048689
JPL HORIZONS	-1.60145	0.44411	0.048592

Additionally, using either method for calculating the position vectors of the planets, the eccentric anomaly can be found. Note that both methods assume that, unlike for the standard two-body problem, the orbital elements of the planets' orbits change in time. Even though such changes are minimal and become more noticeable in an interval of time of the order of centuries, they were still taken into account in the analysis that follows.

Velocity Vectors of Earth and Mars

Once the position vectors of the planets are found, it is necessary to compute the velocity vectors. First, velocity vectors in perifocal coordinates are calculated. As Figure 2 shows, the perifocal coordinate reference frame is defined with the center being the focus (in this case the Sun); by the p-coordinate pointing in the direction of the planet's periapse location, by the w-coordinate pointing normal to the orbital plane such that the planet's motion is counterclockwise and by the q-coordinate which completes the right-handed reference frame. Additionally, $\bar{x}$ and $\bar{y}$ are the components of the distance of the planet from the Sun in the p-direction and q-direction respectively; hence, by Pythagorean Theorem, $r = \sqrt{\bar{x}^2 + \bar{y}^2}$ is the magnitude of the distance.

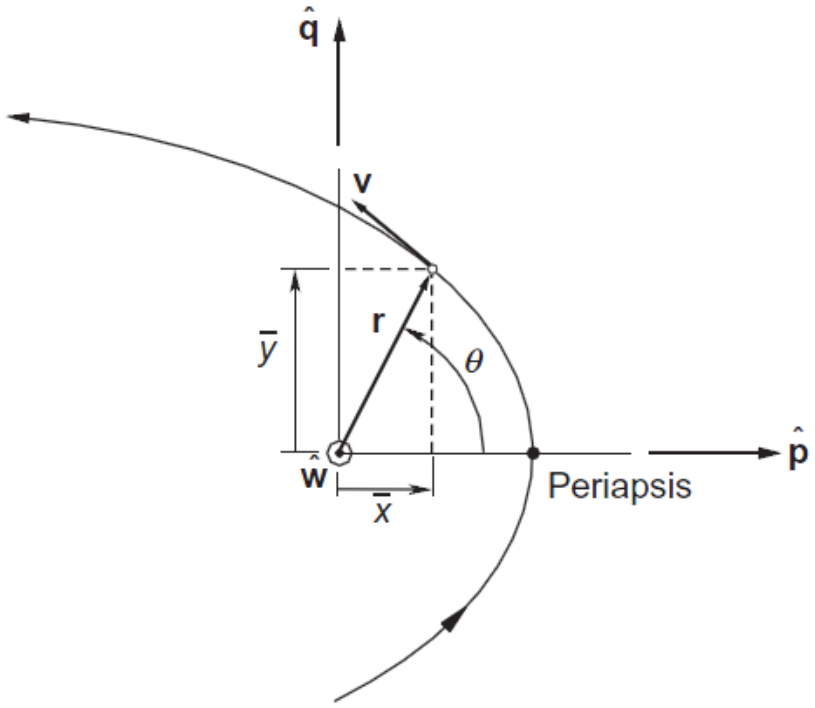

Figure 2 – Position and velocity relative to the pqw perifocal reference frame. Source: Curtis, p. 114.[7]

Successively, a direction cosine matrix can be used to obtain the velocity vectors in J2000 coordinate frame. In perifocal coordinates, the velocity vector of a planet orbiting the Sun is defined as follows:

$$\vec{v}^P = -\sqrt{\frac{\mu_{Sun}}{p}}\sin\theta\ \hat{p} + \sqrt{\frac{\mu_{Sun}}{p}}(e + \cos\theta)\hat{q} \tag{2}$$

where p is semi-latus rectum, θ is true anomaly, e is eccentricity, and μ_{Sun} is the gravitational parameter of the Sun. While μ_{Sun} and e are known, p and θ must be calculated. Given eccentric anomaly E, which was obtained through Standish's algorithm, and knowing semi-major axis a, true anomaly θ and semi-latus rectum p can be calculated:

$$\theta = 2\tan^{-1}\left[\sqrt{\frac{1+e}{1-e}}\tan\left(\frac{E}{2}\right)\right] \tag{3}$$

$$p = a\,(1 - e^2) \tag{4}$$

The direction cosine matrix (DCM) used to convert $\vec{v}^P$ into $\vec{v}^E$ such that $\vec{v}^E = C^{PE}\vec{v}^P$ is given by:

$$C^{PE} = \begin{bmatrix} \cos\Omega\cos\omega - \sin\Omega\sin\omega\cos i & -\cos\Omega\sin\omega - \sin\Omega\cos\omega\cos i & \sin\Omega\sin i \\ \sin\Omega\cos\omega + \cos\Omega\sin\omega\cos i & -\sin\Omega\sin\omega + \cos\Omega\cos\omega\cos i & -\cos\Omega\sin i \\ \sin\omega\sin i & \cos\omega\sin i & \cos i \end{bmatrix} \tag{5}$$

Note that once the perifocal frame is determined, Eq. (5) is the DCM used to convert from perifocal to J2000 ecliptic reference frame. Therefore, the velocity vectors can now be rewritten in the J2000 ecliptic reference frame as:

$$\vec{v}^E = v_x\hat{I} + v_y\hat{J} + v_z\hat{K} \tag{6}$$

Table 2 shows a comparison between the velocity x,y, and z components obtained using Standish's algorithm and those obtained from JPL HORIZONS.

Table 2 - Comparison between velocity vectors of Earth and Mars using Standish's algorithm and using JPL HORIZONS; note that the z-component is considerably smaller than the x and y components.

Earth's Velocity (km/s) on January 22, 2014 at 00:00:00.0 (UT)			
	v_x	v_y	v_z
Standish's algorithm	-25.8345	-15.7563	-0.00050470
JPL HORIZONS	-25.8265	-15.7390	-0.00066392
Mars' Velocity (km/s) on January 22, 2014 at 00:00:00.0 (UT)			
	v_x	v_y	v_z
Standish's algorithm	-5.59172	-21.2728	-0.50470
JPL HORIZONS	-5.58394	-21.2665	-0.30861

Given a departure date from Earth and an arrival date at Mars, it is the possible to determine what the planets' position and velocities would be on those days. This information will be used to solve Lambert's problem as explained in the following chapter.

Chapter 3

Lambert's Problem

In order to determine the transfer trajectory orbital parameters and the necessary ΔVs to accomplish such transfer, it is essential to solve Lambert's Problem. In astrodynamics, Lambert's problem is a two-point boundary value problem (see Figure 3) for the following governing equation of motion:

$$\ddot{\boldsymbol{r}} = -\frac{\mu \boldsymbol{r}}{r^3} \tag{7}$$

In the case of an Earth to Mars transfer, the boundary conditions become:

$$\vec{r}_1(t_1) = \vec{r}\left(t_{departure}\right) = \vec{r}_{Earth} \tag{8}$$

$$\vec{r}_2(t_2) = \vec{r}(t_{arrival}) = \vec{r}_{Mars} \tag{9}$$

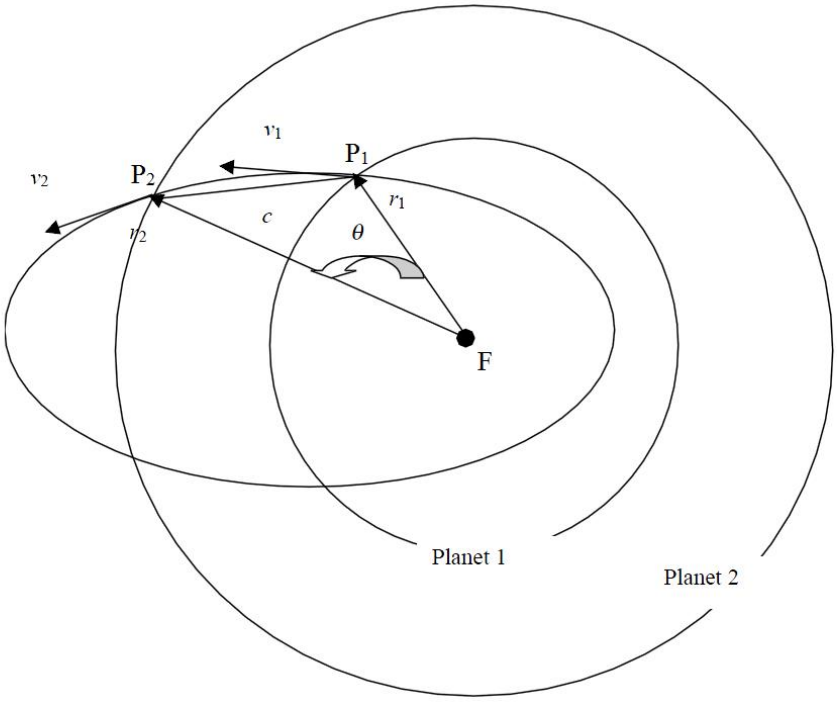

Figure 3 – Geometry of Lambert problem for an interplanetary trajectory. Source: Kemble, p. 9.[9]

The innovative conjecture Lambert had developed is based on geometric reasoning. In fact, Lambert believed that the time required to transverse an elliptic arc between two points depends only on the size of the orbit, i.e.semimajor axis a, on the chord length c and the sum of the radii from the focus to points P_1 and P_2, or $r_1 + r_2$. Mathematically, this can be expressed as follows:

$$t_2 - t_1 = f(a, c, r_1 + r_2) \tag{10}$$

Starting from Kepler's equation, Eq. (11), it is possible to derive an equation, sometimes called Lambert's equation, Eq. (12), that does not depend on eccentricity and that is used to solve Lambert's Problem. Such derivation can be found in most astrodynamics textbooks such as Orbital Mechanics by Prussing and Conway, pages 67-70. [10]

$$E_2 - E_1 - e(\sin E_2 - \sin E_1) = \sqrt{\frac{\mu}{a^3}}(t_2 - t_1) \tag{11}$$

$$a^{3/2}[\alpha - \sin\alpha - (\beta - \sin\beta)] = \sqrt{\mu}(t_2 - t_1) \tag{12}$$

In Eq. (12), the unknown to solve for is semimajor axis a while α and β are defined as:

$$\sin\left(\frac{\alpha}{2}\right) = \left(\frac{s}{2a}\right)^{1/2} \tag{13}$$

$$\sin\left(\frac{\beta}{2}\right) = \left(\frac{s-c}{2a}\right)^{1/2} \tag{14}$$

$$s = \frac{1}{2}(r_1 + r_2 + c) \tag{15}$$

$$c = \sqrt{{r_1}^2 + {r_2}^2 - r_1 r_2 \cos\Delta\theta} \tag{16}$$

$$\Delta\theta = \begin{cases} \cos^{-1}\left(\frac{\vec{r}_1 \cdot \vec{r}_2}{r_1 r_2}\right) & if\ \left[(\vec{r}_1 x\, \vec{r}_2)\cdot \hat{K}\right] \geq 0 \\ 2\pi - \cos^{-1}\left(\frac{\vec{r}_1 \cdot \vec{r}_2}{r_1 r_2}\right) & if\ \left[(\vec{r}_1 x\, \vec{r}_2)\cdot \hat{K}\right] < 0 \end{cases}$$

(17)

Note that, given the definitions of α, β and s, it can be seen that, as expected, Eq. (12) depends only on a, c, and $r_1 + r_2$.

Derivation of Lambert's Problem Solution Using the Universal Variable

The solution to Lambert's Problem gives the departure and arrival velocity vectors, $\vec{v}_1$ and $\vec{v}_2$ in Figure 3, that an arbitrary spacecraft needs to achieve in order to perform the transfer trajectory from P_1 to P_2 for a given amount of time. In this analysis, Lambert's Problem was applied to the heliocentric cruise neglecting the sizes of the departure and arrival planets' spheres of influence. Additionally, only prograde orbital transfers were considered.

In order to obtain $\vec{v}_1$ and $\vec{v}_2$ in the J2000 ecliptic reference frame, Langrange coefficients can be used. In fact, starting from the general relationship involving Lagrange coefficients f, $\dot{f}$, g, $\dot{g}$

$$\begin{Bmatrix} \vec{r}_2 \\ \vec{v}_2 \end{Bmatrix} = \begin{bmatrix} f & g \\ \dot{f} & \dot{g} \end{bmatrix} \begin{Bmatrix} \vec{r}_1 \\ \vec{v}_1 \end{Bmatrix} \tag{18}$$

the velocities $\vec{v}_1$ and $\vec{v}_2$ can be expressed as functions of the boundary conditions (i.e. the position vectors $\vec{r}_1$ and $\vec{r}_2$) as follows:

$$\vec{v}_1 = \frac{1}{g}(\vec{r}_2 - f\vec{r}_1) \tag{19}$$

$$\vec{v}_2 = \frac{1}{g}(\dot{g}\vec{r}_2 - \vec{r}_1) \tag{20}$$

The Lagrange coefficients can be found using the following relationships. Note that $\vec{v}_1$ and $\vec{v}_2$ do not involve $\dot{f}$. Hence, $\dot{f}$ was not taken into account.

$$f = 1 - \frac{y(z)}{r_1} \tag{21}$$

$$g = A\sqrt{\frac{y(z)}{\mu}} \tag{22}$$

$$\dot{g} = 1 - \frac{y(z)}{r_2} \tag{23}$$

$$A = \pm \sin\Delta\theta \sqrt{\frac{r_1 r_2}{1-\cos\Delta\theta}} \tag{24}$$

$$y(z) = r_1 + r_2 + A\frac{zC_3(z)-1}{\sqrt{C_2(z)}} \tag{25}$$

The sign of A in Eq. (24) is assessed in the next section, 'Minimum Energy Solution.' In Eq. (25), $C_3(z)$ and $C_2(z)$ are Stumpff functions and are defined by the following expressions:

$$C_2(z) = \begin{cases} \frac{1-\cos\sqrt{z}}{z} & if\ z > 0 \\ \frac{\cosh\sqrt{-z}-1}{-z} & if\ z < 0 \\ \frac{1}{2} & if\ z = 0 \end{cases} \tag{26}$$

$$C_3(z) = \begin{cases} \frac{\sqrt{z}-\sin\sqrt{z}}{z^{3/2}} & if\ z > 0 \\ \frac{\sin\sqrt{-z}-\sqrt{-z}}{(-z)^{3/2}} & if\ z < 0 \\ \frac{1}{6} & if\ z = 0 \end{cases} \tag{27}$$

Moreover, z is a variable defined as

$$z = \tilde{\alpha}\chi^2 \tag{28}$$

$$\tilde{\alpha} = \frac{1}{a} \tag{29}$$

In order to solve for the value of z, it is necessary to find the zeroes of the following transcendental function:

$$F(z) = \left[\frac{y(z)}{C_2(z)}\right]^{3/2} C_3(z) + A\sqrt{y(z)} - \sqrt{\mu}(t_2 - t_1) \tag{30}$$

i.e. solving the equation $F(z) = 0$, which can be done by using a root finding method such as the Newton-Raphson method. Once a guess on the initial value of z is made, then the following equation can be solved iteratively until a certain relative tolerance is satisfied:

$$z_{i+1} = z_i - F(z_i)/F'(z_i) \tag{31}$$

Here, $F'(z_i) = \frac{\partial F(z_i)}{\partial z_i}$. Note that a good initial guess for z would be $z = 0$. Additionally, in Eq. (28) χ is known as the universal variable. Using χ when solving Lambert's problem is preferable because it avoids encountering discontinuities when iterating to solve for z. In fact, the solution to Lambert's problem can yield an elliptical or hyperbolic transfer trajectory, depending on the given departure and arrival times. Because of this fact, while iterating to solve for z, the value of

semimajor axis a could vary between positive, negative, and undefined. If "regular variables" instead of the universal variable were to be used, this latter possible value that a could attain would cause the iterative process for finding z to be inconclusive. Therefore, no solution for the Lambert's Problem would be found.

Once the value of z is determined within a certain tolerance, then the velocity vectors $\vec{v}_1$ and $\vec{v}_2$ can be computed using the Lagrange coefficients as mentioned previously. The next sections present a special case of the minimal energy Lambert's Problem solution and a summarized step-by-step algorithm for solving the Lambert's Problem.

Minimum Energy Solution

Additionally, in order to resolve the sign of Eq. (24), the minimum energy transfer must be assessed. In fact, the minimum transfer energy for the Lambert's solution happens when the characteristic orbital energy $\varepsilon = -\frac{\mu}{2a}$ is minimum. It can be shown that ε is minimized when

$$a_m = \frac{s}{2} \tag{32}$$

Note that the subscript *m* stands for "minimum." Substituting Eq. (32) into Eq. (13) and solving for α yields to $\alpha_m = \pi$. Using this value for α_m in Eq. (14) and solving for β results in $\beta_m = 2\sin^{-1}\sqrt{\frac{s-c}{s}}$. Using α_m and β_m in Eq. (12) permits to solve for $(t_2 - t_1)_m$:

$$\Delta t_m = (t_2 - t_1)_m = \frac{1}{\sqrt{\mu}}\left(\frac{s^3}{8}\right)^{\frac{1}{2}}(\pi - \beta_m + \sin\beta_m) \tag{33}$$

Note that minimizing the energy of the transfer orbit does not result in the minimum time of flight. Additionally, the values for semilatus rectum and eccentricity of the minimum energy transfer can be determined as follows:

$$p_m = \frac{r_1 r_2(1-\cos\Delta\theta)}{c} \tag{34}$$

$$e_m = \sqrt{1 - \frac{p_m}{a_m}} \tag{35}$$

Once the value of Δt_m is determined, then for a given time of flight $(t_2 - t_1)$, A from Eq. (24) can be determined as follows:

$$A = \begin{cases} \sin\Delta\theta \sqrt{\frac{r_1 r_2}{1-\cos\Delta\theta}} & if\ \Delta t_m \geq (t_2 - t_1) \\ -\sin\Delta\theta \sqrt{\frac{r_1 r_2}{1-\cos\Delta\theta}} & if\ \Delta t_m < (t_2 - t_1) \end{cases} \tag{36}$$

Algorithm for Solving Lambert's Problem

This section illustrates a step-by-step algorithm to solve the general case of the Lambert's Problem for an interplanetary transfer from Earth to Mars. Prograde motion is assumed for all possible transfer orbits. Appendix A comprises of a flowchart that illustrates how this algorithm can be implemented in a computer language such as MATLAB in order to make computations such as the iterative process to find z faster.

Solution to Lambert's Problems for given departure and arrival dates:

1. t_{dep} and t_{arr} are given
2. Compute $\vec{r}_{Earth}$, $\vec{r}_{Mars}$, using the method described in Chapter 2.
3. Find the values of $|\vec{r}_{Earth}|$, $|\vec{r}_{Mars}|$ (lengths of the position vectors), chord c, transfer angle $\Delta\theta$, s and A
4. Iterate to get the value of z
5. Solve for $y(z)$
6. Find the Lagrange coefficients: f, g, $\dot{g}$
7. Compute $\vec{v}_1$ and $\vec{v}_2$

Planetary Departure

Once $\vec{v}_1$ and $\vec{v}_2$ are determined via the solution to Lambert's Problem, planetary departure and arrival must be considered. In fact, when setting up Lambert's Problem, the spheres of influence of Earth and Mars were ignored. In reality, before being able to leave Earth's sphere of influence, it is necessary to transit from a parking elliptical orbit about Earth to a hyperbolic orbit as shown in Figure 4.

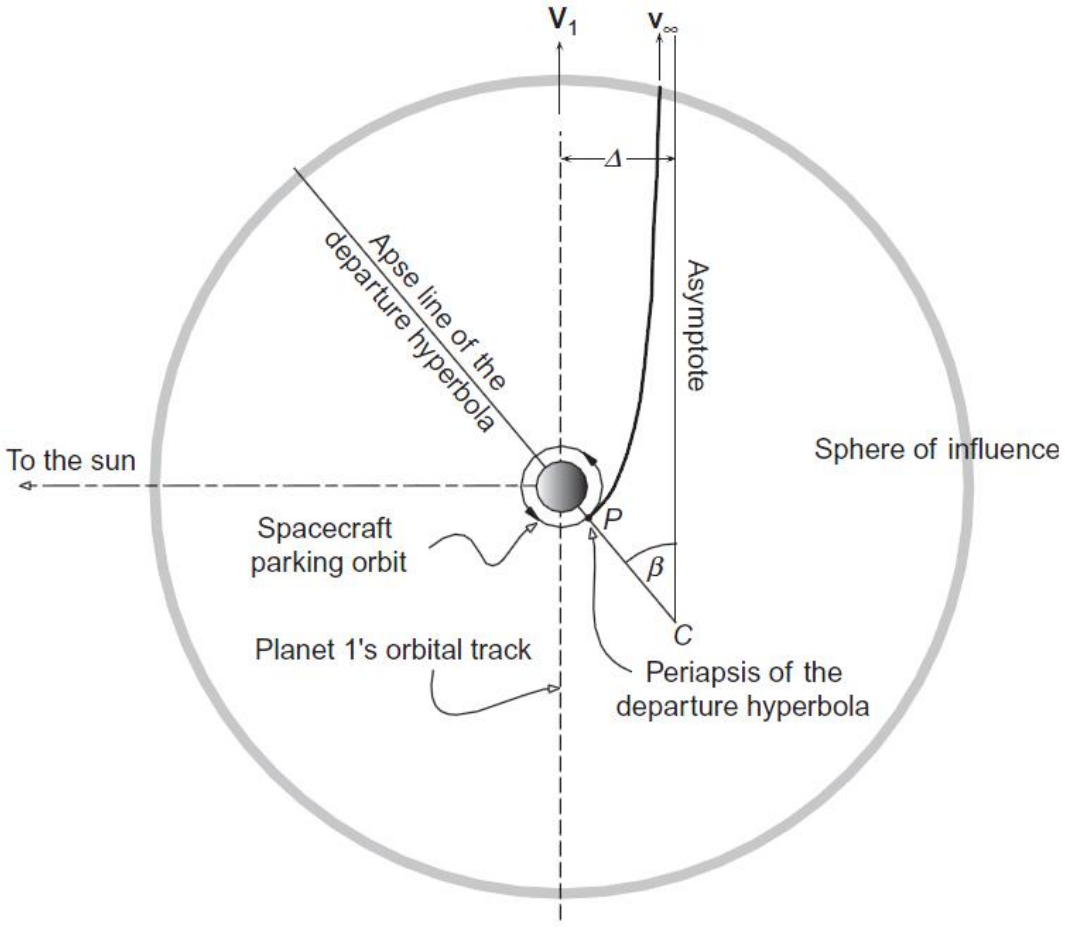

Figure 4 – Departure orbit geometry. Source: Curtis, p. 443.[7]

Hence, the velocity of the spacecraft's hyperbolic orbit at the boundary of the sphere of influence with respect to Earth must be:

$$\vec{v}_{\infty/Earth} = \vec{v}_{sc/Sun,1} - \vec{v}_{Earth/Sun} \tag{37}$$

Here, $\vec{v}_{sc/Sun,1} = \vec{v}_1$ which was calculated from the Lambert's Problem while $\vec{v}_{Earth/Sun} = \vec{v}_{Earth}$ which is the velocity of Earth with respect to the Sun. The latter quantity can be obtained from Standish's algorithm as explained in Chapter 2. Therefore, it is possible to compute $\vec{v}_{\infty/Earth}$ and its magnitude. Additionally, note that Eq. (37) is a vector relation and therefore comparing the various velocity magnitudes does not suffice and is only applicable when all vectors are parallel to each other.

In order to determine the necessary Δv to put the spacecraft onto a hyperbolic trajectory, initial orbital conditions of the spacecraft parking orbit must be given as shown on Figure 4. Assuming a circular parking orbit around the Earth with known altitude h_{Earth}, the velocity of the spacecraft can be calculated as follows:

$$v_{c,Earth} = \sqrt{\frac{\mu_{Earth}}{R_{Earth}+h_{Earth}}} \tag{38}$$

Then, using the vis-viva equation, it is possible to write an energy balance between the parking orbit and the hyperbolic orbit:

$$\frac{\left(v_{\infty/Earth}\right)^2}{2} = \frac{\left(v_{c,Earth}+\Delta v_1\right)^2}{2} - \frac{\mu_{Earth}}{R_{Earth}+h_{Earth}} \tag{39}$$

In Eq. (39) the only unknown is Δv_1. Solving for Δv_1 yields to two different solutions only one of which is positive and is hence the correct answer. Usually, the term $\left(v_{\infty/Earth}\right)^2$ is referred to as $C3$. More generally,

$$C3 = \left(v_{\infty/Departure\ Planet}\right)^2 \tag{40}$$

$C3$ is therefore related to the characteristic energy of the departure hyperbolic orbit. Additionally, $C3$ is a key parameter used in interplanetary trajectory design as discussed in Chapter 4.

Planetary Arrival

After the spacecraft travels from Earth to the sphere of influence of Mars, another maneuver must be performed in order to have the spacecraft be captured by the arrival planet. In fact, as Figure 5 shows, if no Δv_2 is executed the spacecraft would do a flyby of Mars without entering a closed elliptical orbit around it and leaving its sphere of influence on a flyby trajectory.

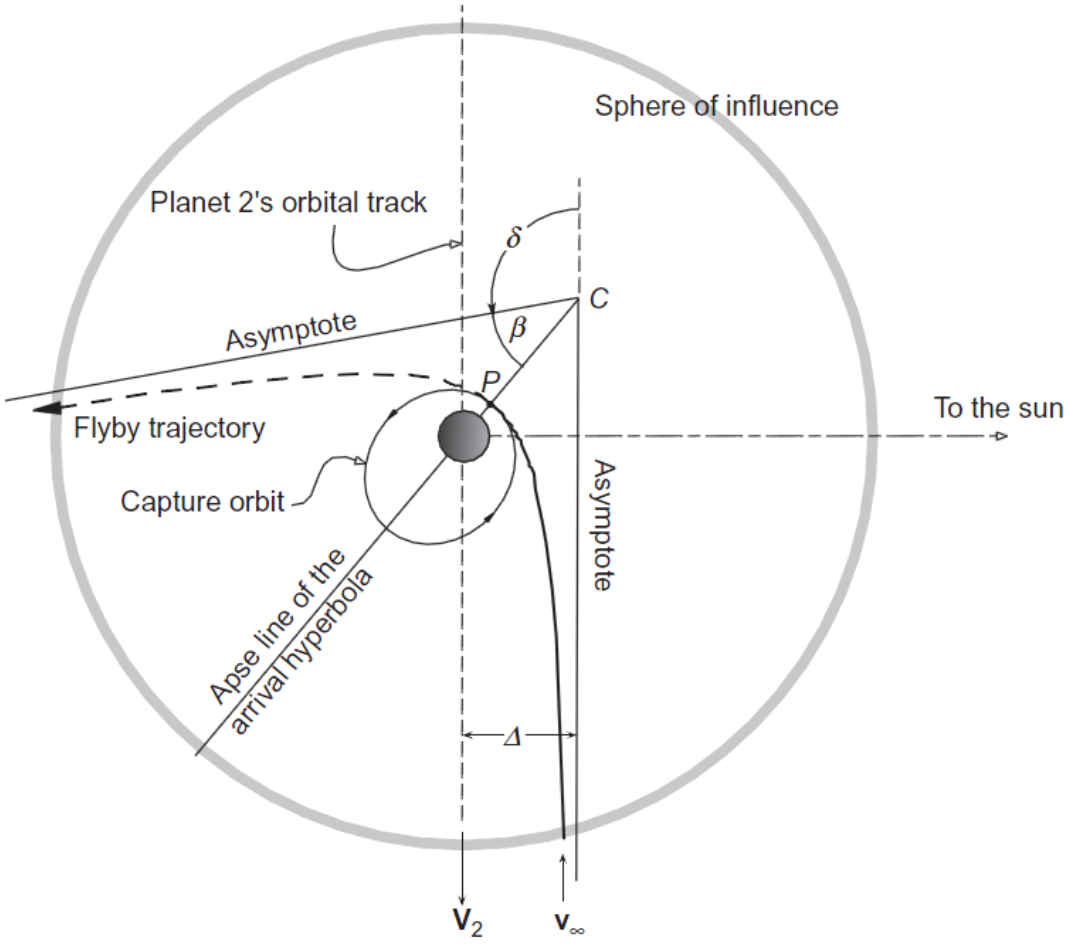

Figure 5 – Planetary approach. Source: Curtis, p. 451.[7]

From the solution to Lambert's Problem, it is possible to obtain $\vec{v}_{\infty/Mars}$ as follows:

$$\vec{v}_{\infty/Mars} = \vec{v}_{sc/Sun,2} - \vec{v}_{Mars/Sun} \tag{41}$$

Similarly to the previous section, $\vec{v}_{sc/Sun,2} = \vec{v}_2$ and $\vec{v}_{Mars/Sun}$ can be computed with the method described in Chapter 2. Thus, after computing $\vec{v}_{\infty/Mars}$ using Eq. (41), it is possible to solve for Δv_2 from the following equation:

$$\frac{(v_{\infty/Mars})^2}{2} = \frac{(v_{c,Mars}+\Delta v_2)^2}{2} - \frac{\mu_{Mars}}{R_{Mars}+h_{Mars}} \tag{42}$$

Note that the above expression is true for a Δv_2 performed at the hyperbolic periapse which corresponds to the desired final spacecraft parking orbit altitude, h_{Mars}. Additionally, $v_{c,Mars}$ can be calculated as follows:

$$v_{c,Mars} = \sqrt{\frac{\mu_{Mars}}{R_{Mars}+h_{Mars}}} \tag{43}$$

In the approach section of the spacecraft journey from Earth to Mars, it should be noted that the main design parameter upon which the rest of a mission is constructed on is $v_{\infty/Mars}$.

Sphere of Influence Considerations

As mentioned in Chapter 1, the spheres of influence of Earth and Mars are considered to be relatively small for the heliocentric transfer and relatively large for the planetary departure and arrival. The formula for computing the radius of the sphere of influence r_{SOI} of a planet in the Solar System is given by:

$$r_{SOI} \approx r_{planet}\left(\frac{\mu_{planet}}{\mu_{Sun}}\right)^{2/5} \tag{44}$$

Here, r_{planet} is the semimajor axis of the planet's orbit around the Sun. A derivation of Eq. (44) can be found in Wiesel on p. 320-322. When calculating r_{SOI} for Earth and Mars, it can be found that:

$$r_{SOI,Earth} \approx 924{,}652\ km\ or\ 145\ body\ radii$$

$$r_{SOI,Mars} \approx 577{,}133\ km\ or\ 170\ body\ radii$$

Hence, the assumptions made about the spheres of influence of Earth and Mars hold, especially if considering the energy balance expression for a hyperbolic to elliptic transfer, or vice-versa:

$$\frac{\left(\vec{v}_{\infty/Planet}\right)^2}{2} - \frac{\mu_{Planet}}{r_{SOI}} = \frac{\left(v_{c,Planet}+\Delta v\right)^2}{2} - \frac{\mu_{Planet}}{R_{Planet}+h_{Planet}} \tag{45}$$

In Eq. (45) it can be noted that the term $-\frac{\mu_{Planet}}{r_{SOI}} \to 0$ as $r_{SOI} \to \infty$ or, for more practical applications, as r_{SOI} becomes large enough. Thus, Eq. (45) can be simplified to:

$$\frac{\left(\vec{v}_{\infty/Planet}\right)^2}{2} = \frac{\left(v_{c,Planet}+\Delta v\right)^2}{2} - \frac{\mu_{Planet}}{R_{Planet}+h_{Planet}} \tag{46}$$

Total ΔV Calculation and Propellant Mass

In order to obtain the total Δv the overall Earth-Mars transfer requires, one can compute such quantity as follows:

$$\Delta v_{tot} = \Delta v_1 + \Delta v_2 \tag{47}$$

Note that Δv_{tot} does not usually represent the total Δv budget for a mission. In fact, other minor maneuvers such as trajectory correction maneuvers were not taken into account in this analysis. Another key mission parameter is represented by propellant mass. A quick estimate of how much propellant is needed for given mission and propulsion system is given by:

$$m_{\,p} = m_{\,1}(1 - e^{-\Delta v_{tot}/v_{ex}}) \tag{48}$$

Here, $m_{\,1}$ represents the initial mass of the spacecraft (payload, structure, and propellant) while v_{ex} is the exhaust velocity of the propulsion system, or:

$$v_{ex} = I_{\,sp} * g_{SL} \tag{49}$$

where g_{SL} is the acceleration due to gravity at sea level on Earth. Without knowing the total mass of the spacecraft, it is still possible to rearrange Eq. (48) and solve for propellant mass as a percentage of the total mass:

$$\left(\frac{m_p}{m_1}\right)_{percentage} = \left(1 - e^{-\frac{\Delta v_{tot}}{v_{ex}}}\right) * 100\% \quad (50)$$

Examples of Δv and $\left(\frac{m_p}{m_1}\right)_{percentage}$ for a give set of departure and arrival dates are given in Chapter 4.

Chapter 4

Porkchop Plots

Porkchop plots are computer-generated contour plots that display launch dates vs. arrival dates for characteristics of an interplanetary flight path for a given launch and arrival opportunity between two planets within the Solar System[6]. Perhaps the most important characteristics of porkchop plots are $C3$ at departure (or $CL3$) and v_∞ at arrival. In fact, by looking at a porkchop plot it is possible to choose the launch and arrival windows given specific spacecraft performance such as Δv and I_{sp}. Figure 6 shows an example of a porkchop plot where contour lines of constant $C3$ and arrival v_∞ are displayed in red and blue respectively. Additionally, lines of constant time of flight are shown in green. Porkchop plots can be obtained by solving Lambert's Problem for all the possible combination of departure vs. arrival dates provided that no arrival date is earlier than any departure date. Because such task is computationally time consuming, using a computer program such as MATLAB is essential. A flowchart in Appendix B shows how the solution to the Lambert's Problem algorithm presented in Chapter 3 can be expanded in order to create porkchop plots.

Considering the porkchop plot of Figure 6, one can pick departure and arrival dates, say July 30, 2020 and February 5, 2021 respectively, to determine some of the key parameters of the resulting orbital transfer. The two dates (the two dotted lines in Figure 6) define a specific point on the graph which, for convenience, was denoted by an orange dot. From the graph, it is visible that the orange dot lies close to the 14-level red line and the 2.7-level blue line. According to the plot legend, this means that for this particular combination of dates, $CL3 \approx 14\ km^2/s^2$ and $v_\infty \approx 2.7\ km/s$. Additionally, it is possible to estimate the time of flight to be about 190 days since the

dot lies slightly below the 200-level green line. In other words, for this 190 day transfer a characteristic energy of about 14 km^2/s^2 must be reached by the spacecraft as it is leaving Earth's sphere of influence; also, upon arrival to Mars, the spacecraft would enter Mars' sphere of influence with a speed of approximately 2.7 km/s. Note that in order to know more accurate results for $CL3$, v_∞ and time of flight, it is necessary to consult the numerical results that MATLAB gives.

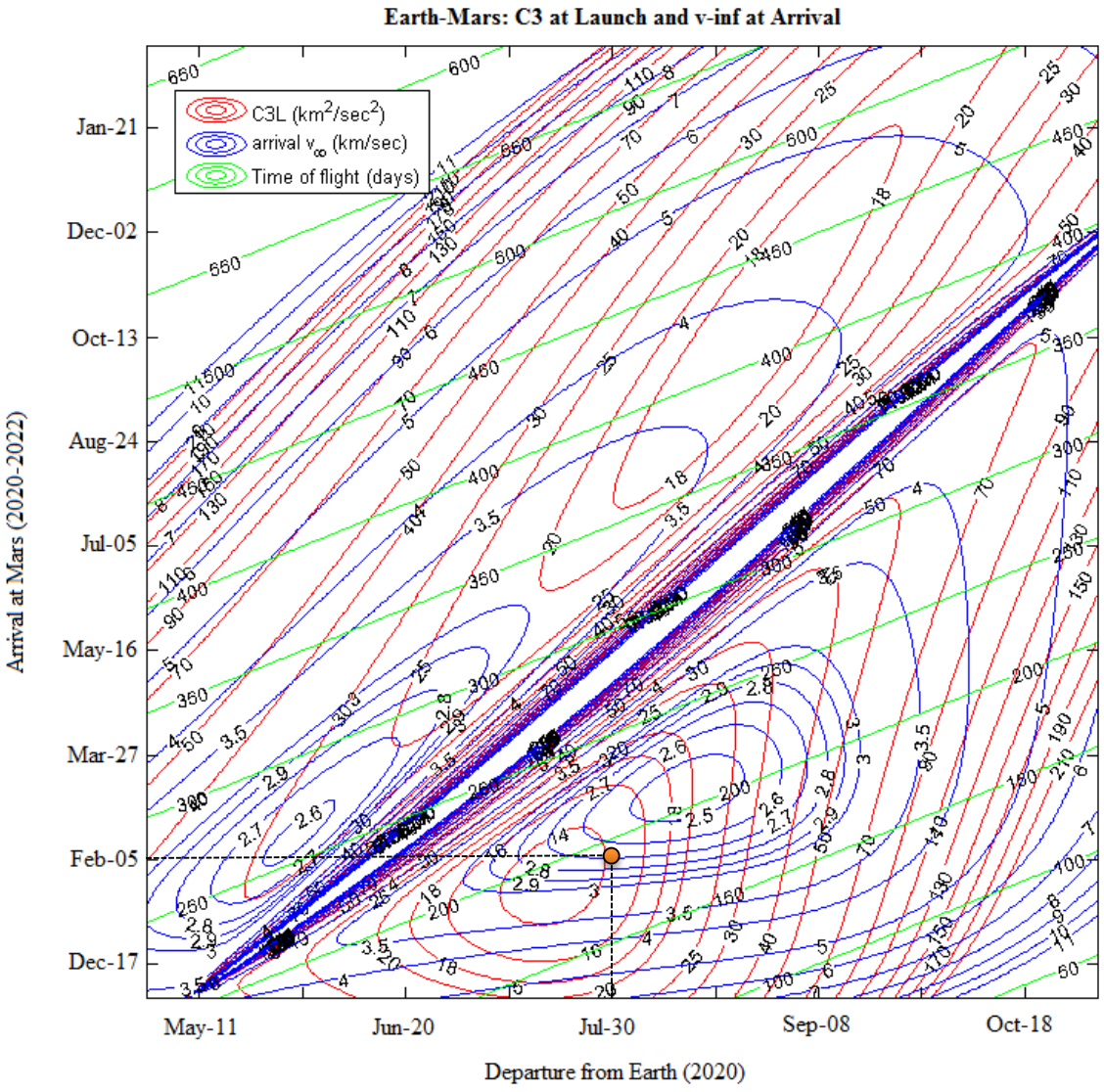

Figure 6 – Porkchop plot for the years 2020-2022 timeframe. The orange dot represents the sample point used in this section to explain how to read a porkchop plot.

Key Features of a Porkchop Plot

One of the key features of porkchop plots is the presence of a singularity shown on the plot as a diagonal line usually going from the bottom left corner to the upper right corner where the values of $C3$ and arrival v_∞ get extremely large. This singularity is due to the fact that 0 and, most importantly, 180 degree transfers (i.e. $\Delta\theta = 0°$ and $\Delta\theta = 180°$) make the transfer plane between departure and arrival undefined as explained in Chapter 6. Because of this fact, solutions of Lambert's Problem close to the singularity give unpractical results for interplanetary trajectory design. Additionally, this singularity divides the possible transfer orbits into two main classes: type I transfers and type II transfers. The former are defined for having $0° < \Delta\theta < 180°$ and are found in the region bounded above by the singularity diagonal; the latter are defined for having $180° < \Delta\theta < 360°$ and are found in the region bounded below by the singularity diagonal. Examples of type I and type II transfers are shown in Figure 7 and Figure 8 respectively. Note that in these figures blue, red and green represent Earth's orbit, Mars' orbit, and the transfer orbit Earth-Mars respectively.

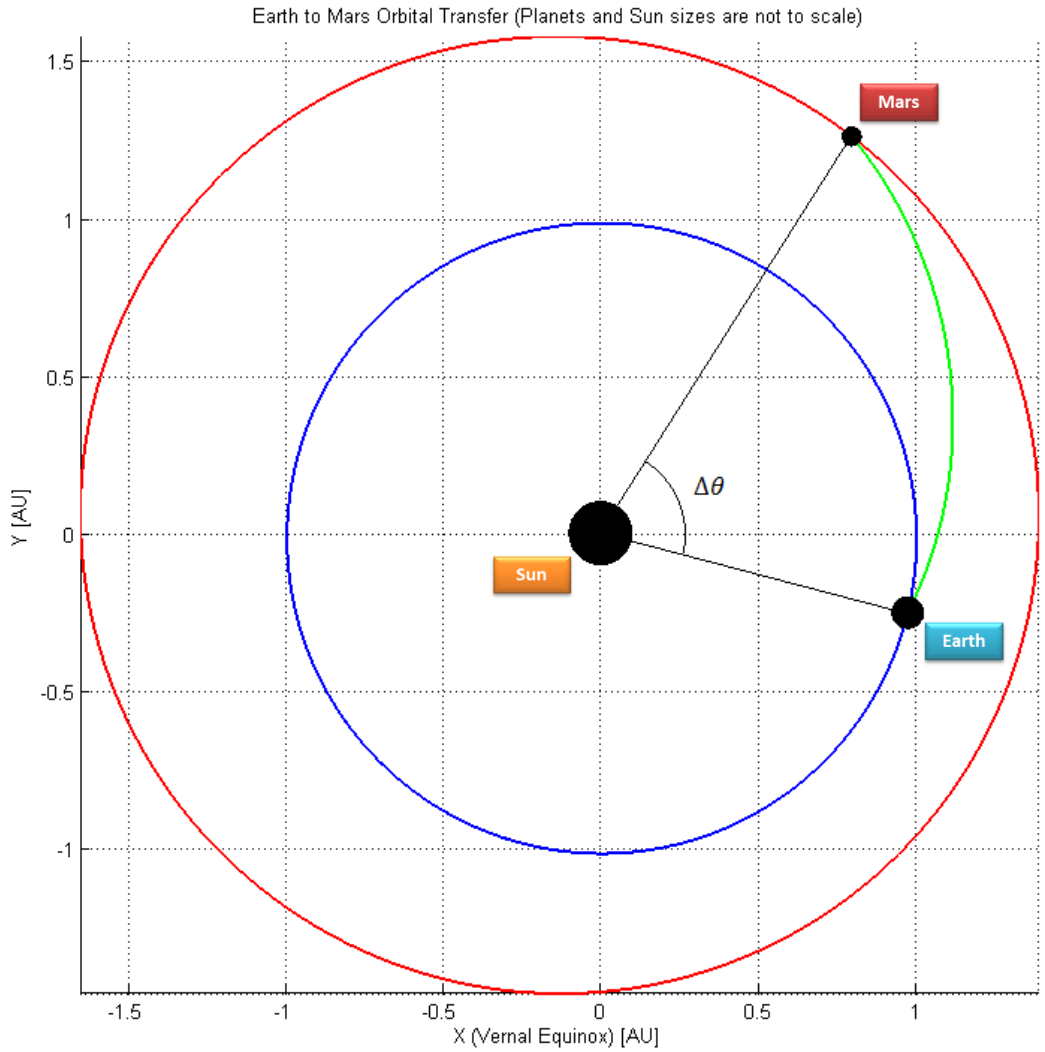

Figure 7 – Example of a Type I transfer with launch on September 8, 2020 and arrival on December 17, 2020.

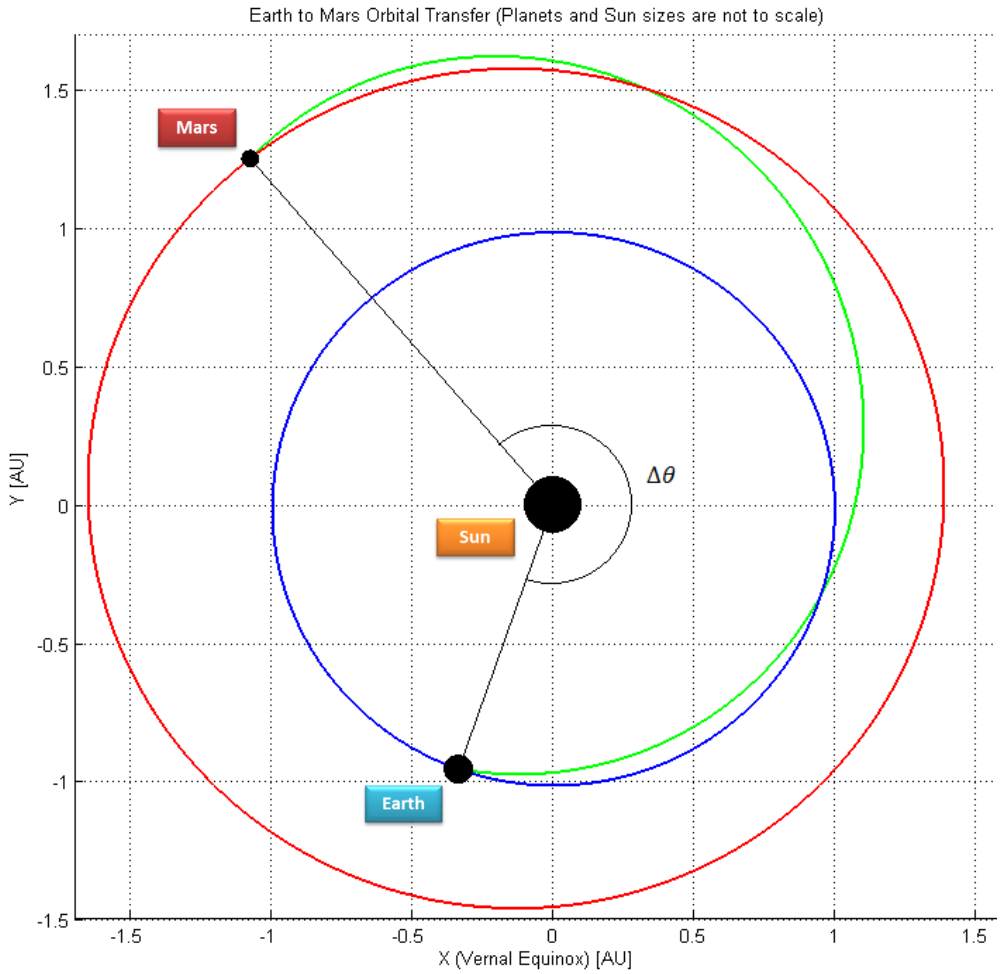

Figure 8 – Example of a Type II transfer with launch on June 1, 2020 and arrival on May 16, 2021.

ΔV vs. Departure Date vs. Arrival Date

Once $C3$ at departure and v_∞ at arrival have been calculated for all the possible combinations of dates of interest, as explained in Chapter 3, it is possible to calculate Δv_1 and Δv_2 using Eq. (39) and Eq. (42). Then, using Eq. (47), Δv_{tot} can be found for all the range of dates. Figure 9 shows a contour plot of Δv_{tot} for the same ranges of dates used for the porkchop plot of Figure 6. In this case, an initial Earth-centered circular parking orbit with an altitude of 300 km and a final Mars-centered circular parking orbit with an altitude of 200 km were considered.

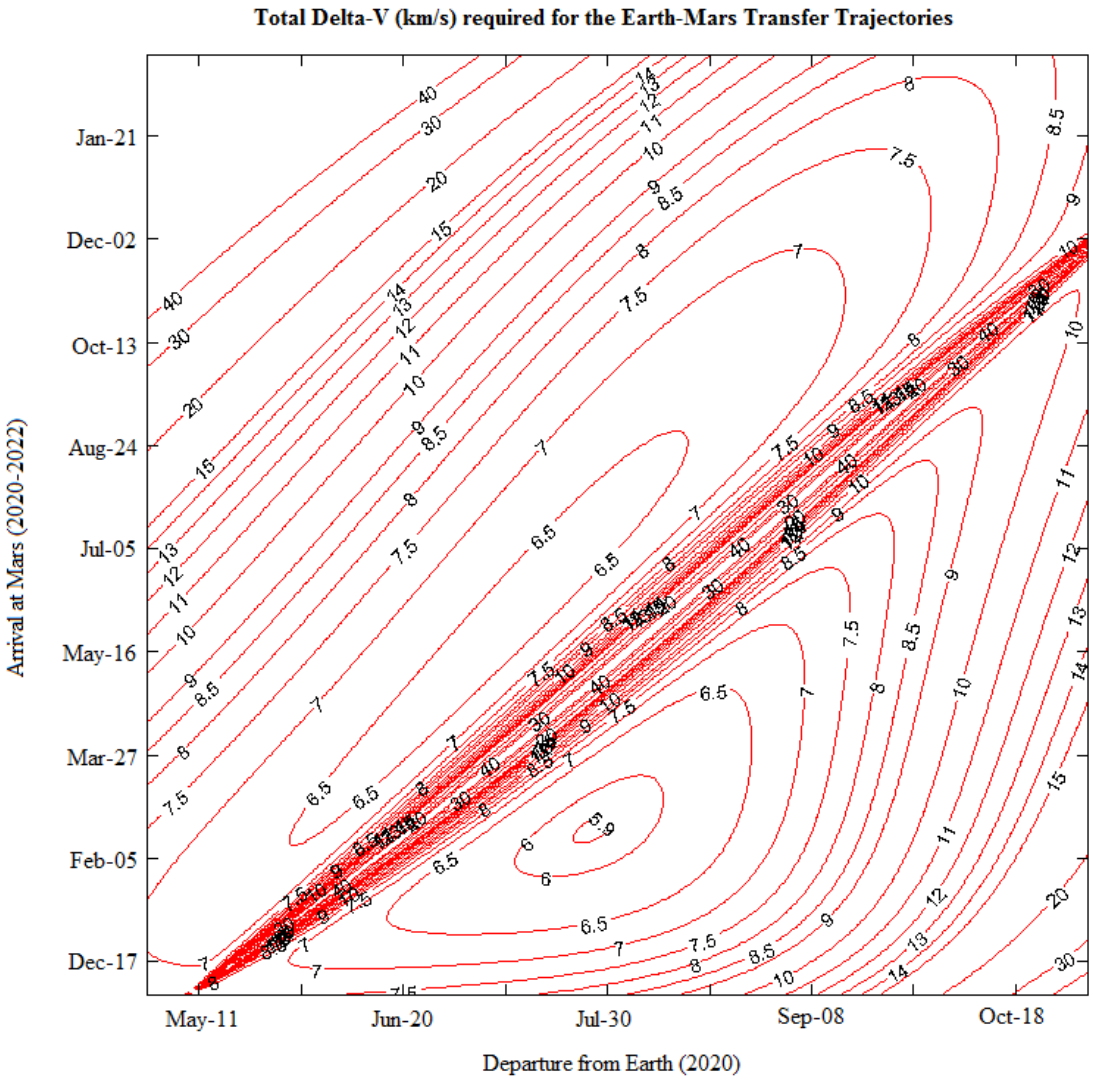

Figure 9 – ΔV_{tot} for the 2020-2022 Earth-Mars transfer trajectories.

From the Δv_{tot} plot the transfer dates that require the least Δv and hence the least amount of propellant can be found. For example, for the 2020-2022 timeframe Figure 9, Table 3 summarizes the key results. Notice that this particular value of Δv_{tot} is a minimum for the type I transfer orbit presented in Figure 9.

Table 3 – Key results of the Earth-Mars trajectory that minimizes ΔV_{tot} in the 2020-2022 timeframe.

Earth-Mars Trajectories for the 2020-2022 timeframe – Minimum ΔV	
Parameter	**Value**
Δv_{tot}	5.8921 km/s
C3 at Launch	14.045 km^2/s^2
v_∞ at Arrival	2.5748 km/s
Departure Date	July 27, 2020
Arrival Date	February 19, 2021
Time of Flight	207 days

Additionally, it is worth noting that the combination of dates at which the minimum Δv_{tot} happens is usually not where the minimum C3 at launch and minimum v_∞ at arrival occur, although lower values of C3 and v_∞ tend to give lower values of Δv_{tot}.

Propellant Mass

Knowing the required Δv_{tot} for the interplanetary transfer, propellant mass as a percentage of the total spacecraft mass can be easily obtained using Eq. (50). Additionally, as mentioned in Chapter 3, the I_{sp} of the propulsion system used for the main mission transfer must also be known (or estimated). Using an I_{sp} of 350 seconds and considering the 2020-2022 timeframe results into Figure 10. Notice that, as expected, the minimum propellant mass required occurs where the minimum Δv_{tot} occurs.

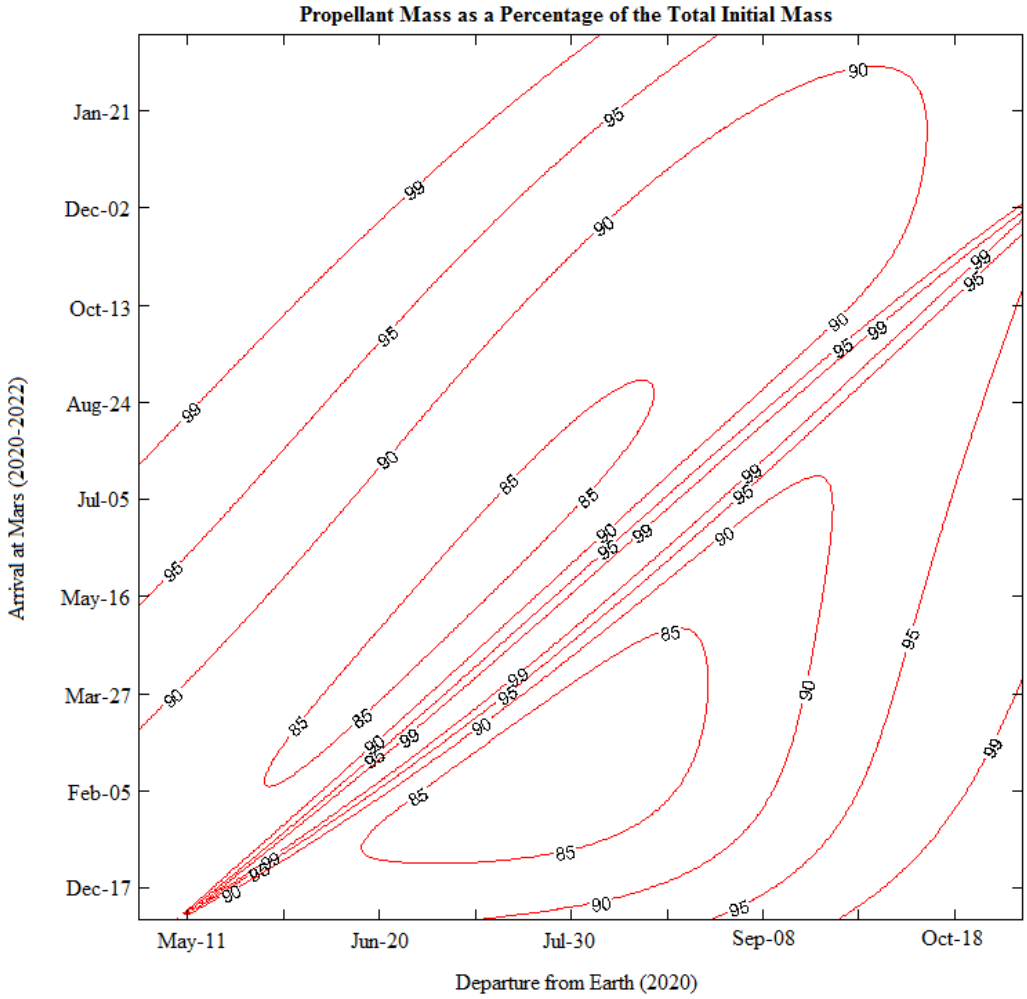

Figure 10 – Propellant mass as a percentage of total initial mass for the 2020-2022 timeframe.

Chapter 5

Orbital Parameters of the Transfer Trajectories and Examples

In order to obtain additional information on the transfer trajectories, such as maximum and minimum distances from the Sun and inclination relative to the ecliptic plane, the orbital parameters of the transfer trajectories must be calculated. Recall that the five classical orbital elements are semimajor axis a, eccentricity e, inclination i, right ascension of the ascending node Ω, and argument of periapse ω. Also, for the two-body problem, from the position and velocity vectors at a specific times it is possible to compute all of the five orbital elements for that particular trajectory. Amongst the orbital elements, those of most interest for this analysis are a, e, and i.

Eccentricity

Eccentricity represents a key parameter especially when considering both elliptical ($0 < e < 1$) and hyperbolic ($e > 1$) transfer trajectories. For given Earth-Mars geometry, spacecraft sent on hyperbolic trajectories from Earth to Mars would arrival at Mars faster than elliptical orbits. An unmanned spacecraft may not be required to reach Mars within a specific time constraint, elliptical orbits are preferred. On the other hand, a manned mission would be more likely to travel on much faster trajectory, particularly to avoid astronauts from being exposed to interplanetary radiation for long periods of time. Therefore, trajectories with $e > 1$ should also be

considered. Figure 11 shows examples of elliptical-only trajectories while

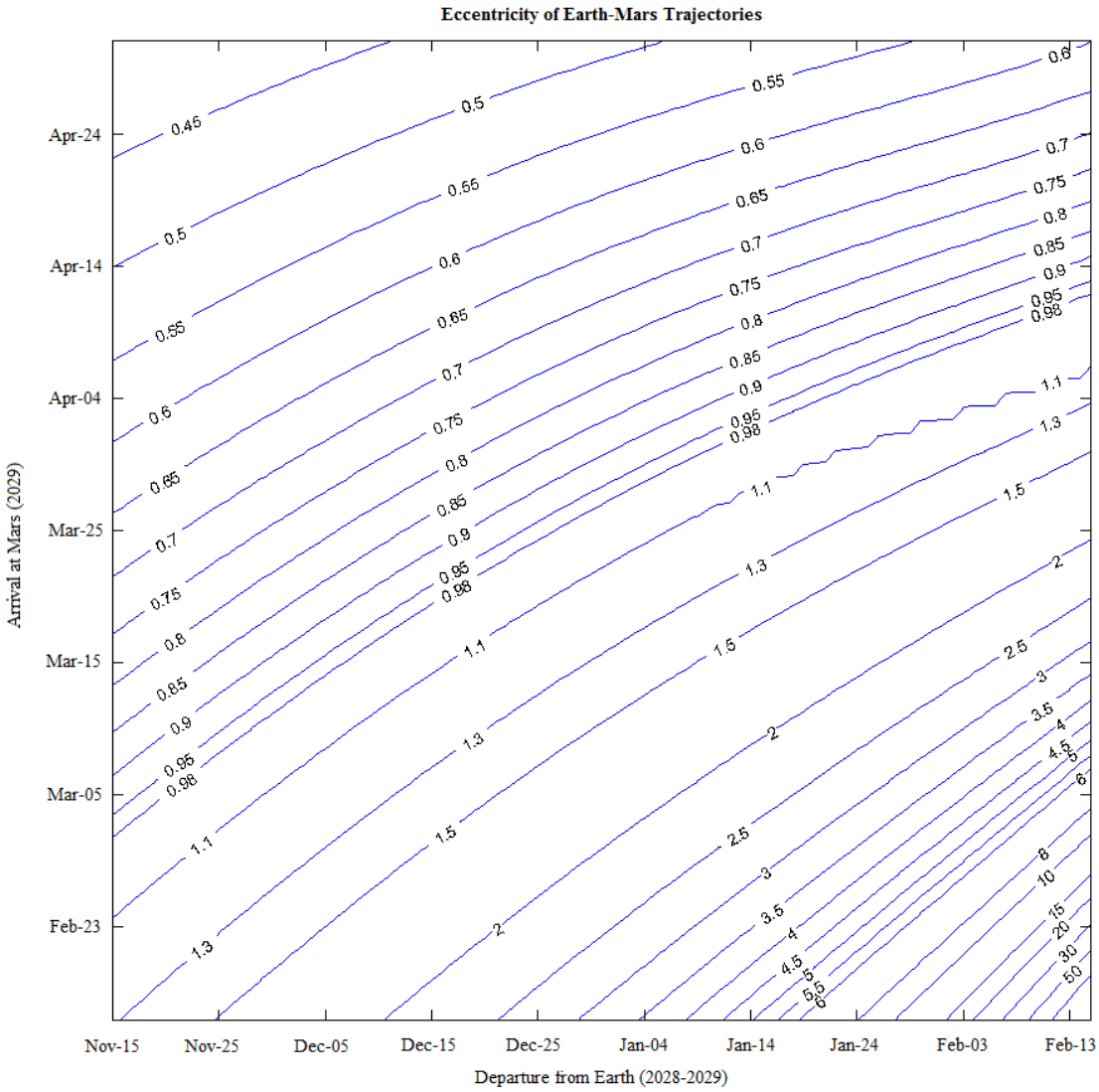

Figure 12 gives examples where $e > 1$.

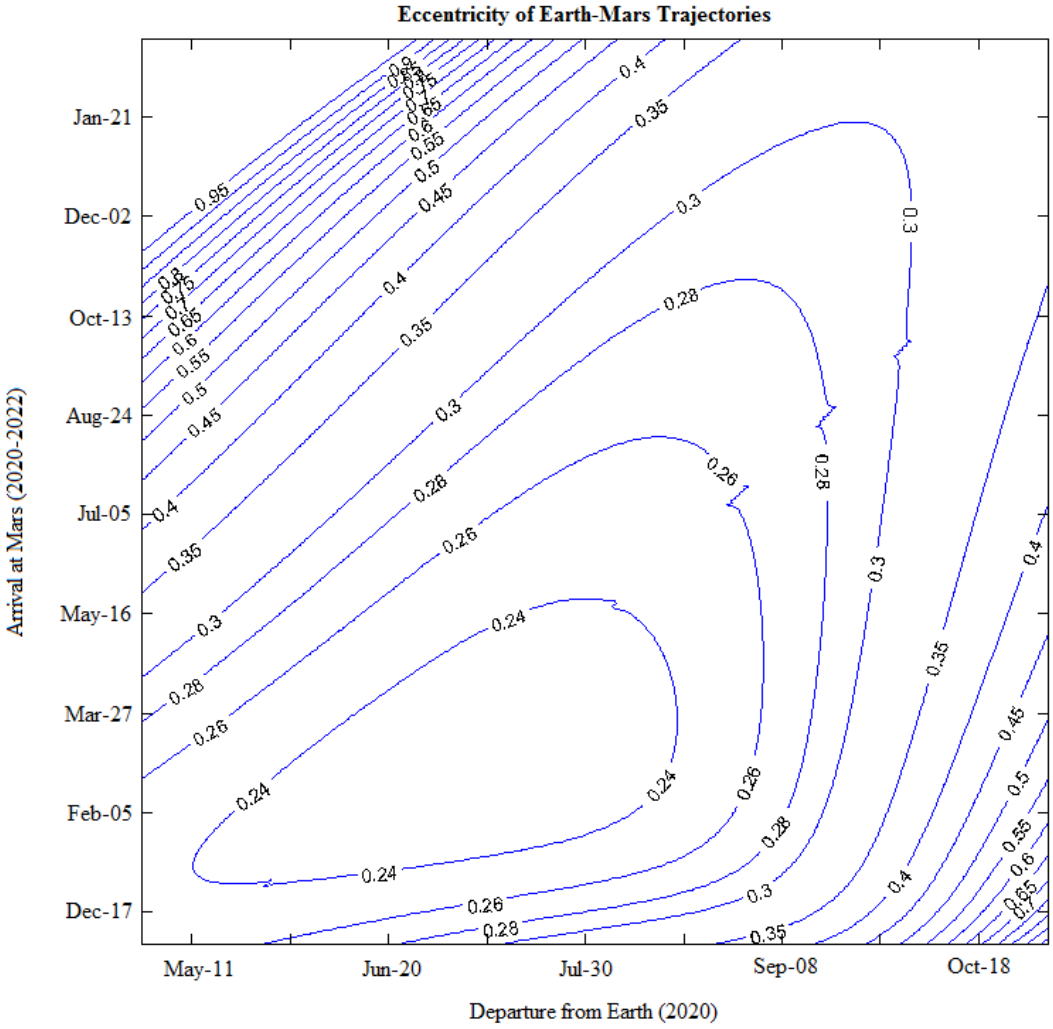

Figure 11 – Example of Earth-Mars trajectories with e < 1.

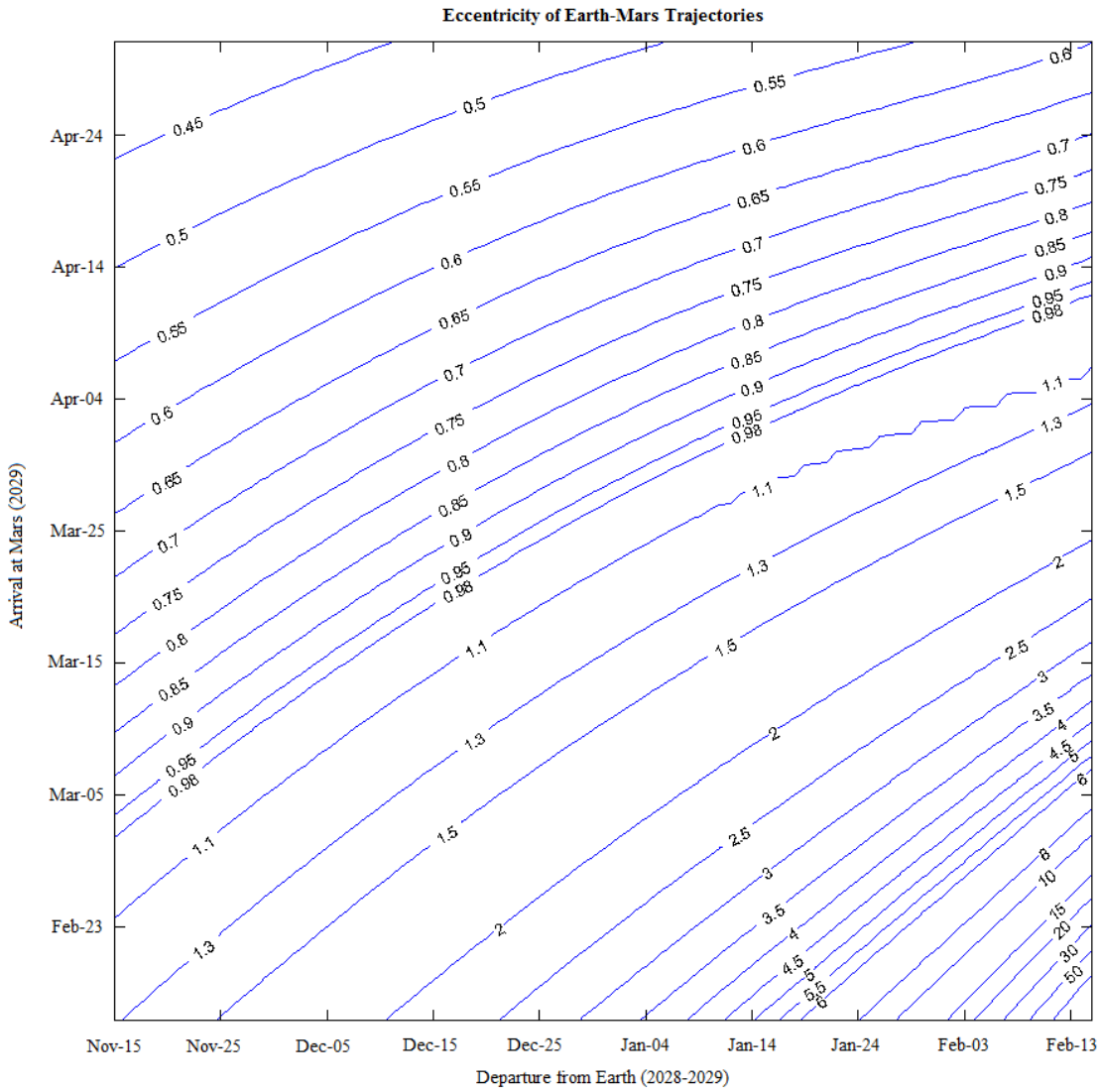

Figure 12 – Example of Earth-Mars trajectories including e > 1.

Semimajor Axis

In order to determine the size of the transfer orbit, semimajor axis a must be known. Additionally, a can be used in combination with e to calculate the maximum and minimum distance from the Sun, i.e. apoapsis and periapsis distances respectively, as follows:

$$r_{apoapse} = a(1 + e) \tag{51}$$

$$r_{periapse} = a(1 - e) \tag{52}$$

If, for example, a spacecraft relies primarily on solar power, it is necessary to know what the furthest distance from the Sun will be in order to be able to correctly size its solar panels. On the other hand, it is also important to know the minimum distance because if, for example, a mission where to use a particular transfer that gets much closer to the Sun than Earth is, the spacecraft involved in such mission may require additional radiation shielding. Figure 13 shows an example of various semimajor axis for a given set of dates.

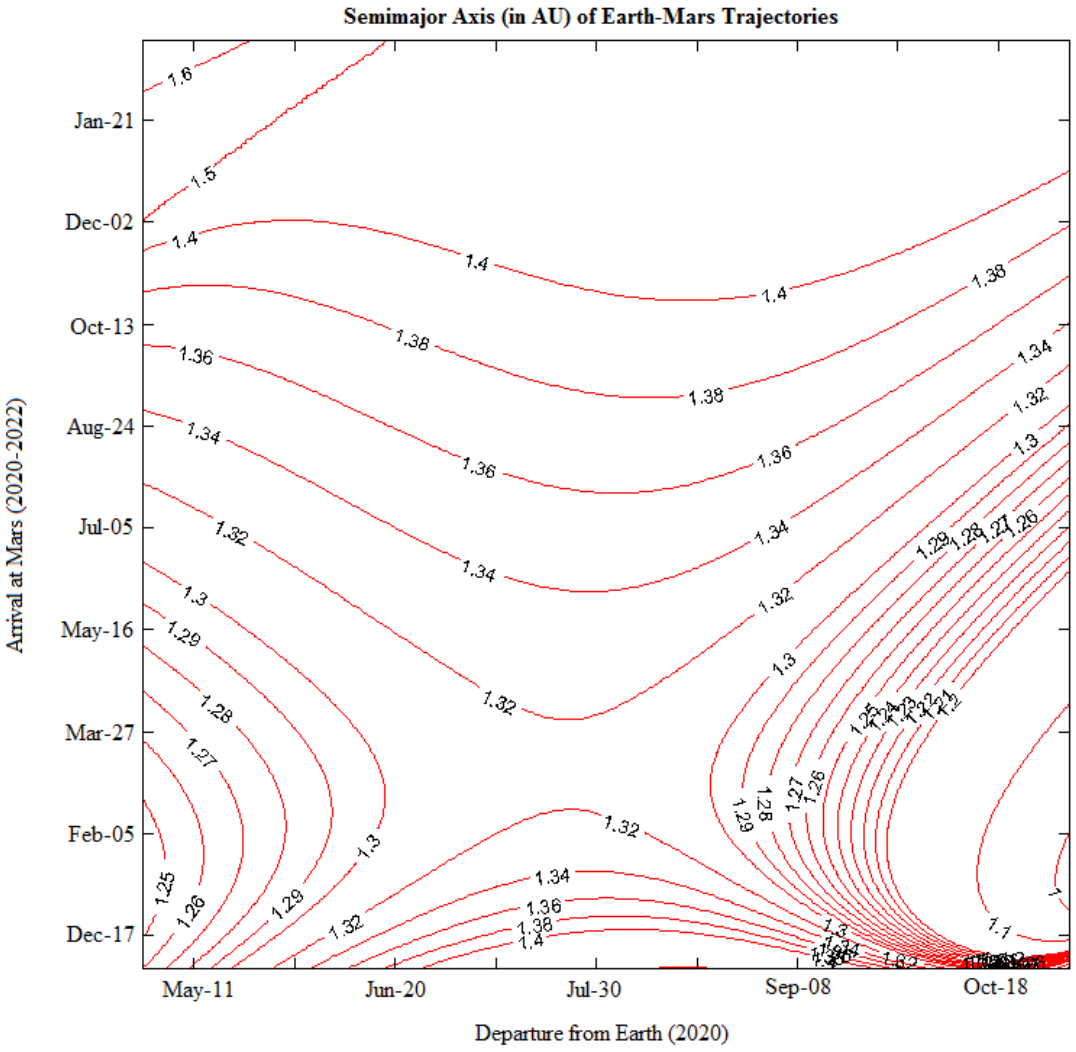

Figure 13 – Example of various semimajor axes for Earth-Mars trajectories

Inclination

Because Earth's and Mars' orbits are relative inclination is small, transfer orbits from Earth to Mars are also expected to have a small inclination as Figure 14 suggests for most of the departure-arrival combinations. Notice that as the date combinations approach the singularity discussed in the porkchop plot section, the inclinations of the transfer orbits increase reaching values in the range of $60° - 80°$. This is due to the fact that as $\Delta\theta \to 0°$ and as $\Delta\theta \to 180°$ the orbital plane becomes undefined. In fact, the Sun, Earth, and Mars can be treated as three points in a three-dimensional space that define a plane, namely the orbital plane of the transfer orbit. When the two planets and the Sun are close to being lined up, the transfer planes take on inclination values that would not be practical for an actual mission and that would require very large amounts of propellant.

In the realm of numerical solutions, it is nearly impossible to get a combination of departure-arrival dates that would give exactly $\Delta\theta = 0°$ or $\Delta\theta = 180°$. On the other hand, values of $\Delta\theta$ that are close enough to $0°$ or $180°$ can make the variable A, which is defined by Eq. (24), become extremely large which yields to the large values of $C3$ at launch and arrival v_∞ as previously discussed. Figure 15 and Figure 16 show cases of orbital transfers with relatively high inclination. In particular, Figure 16 is a case of a nearly $90°$ inclination. Such transfers are not reasonable because they require spacecraft to reach extremely high out-of-plane v_∞ with respect to Earth (hence high values of $C3$) and they also do not fully take advantage of Earth's orbital velocity. Therefore, getting a high inclination transfer as a result from Lambert's problem is a signal that, as discussed later, the solution to Lambert's problem fails to give a reasonable answer. Lastly, as discussed in Chapter 6, reasonable solutions for $\Delta\theta = 180°$ exist and are referred to as Hohmann transfers.

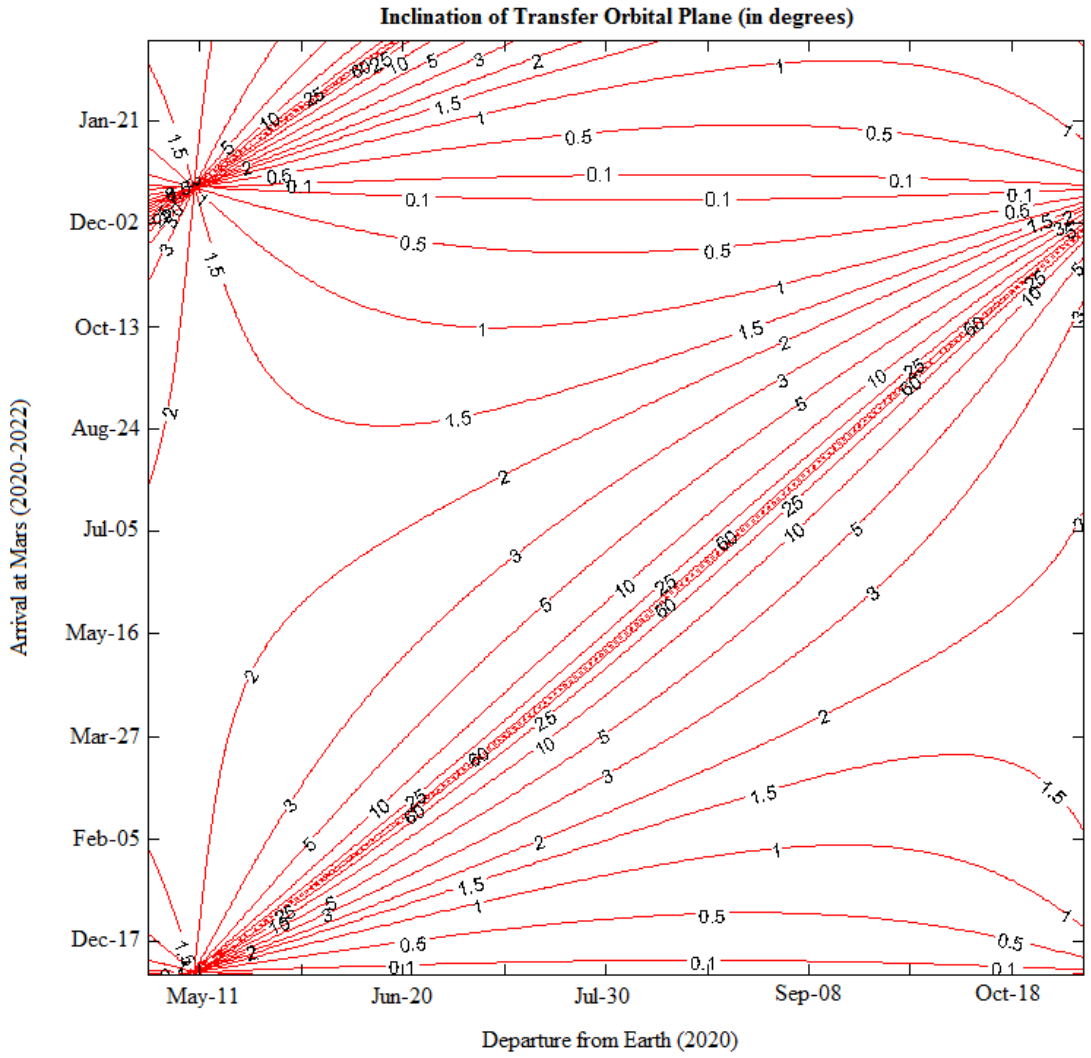

Figure 14 – Inclination of the transfer orbital plane for various Earth-Mars trajectories

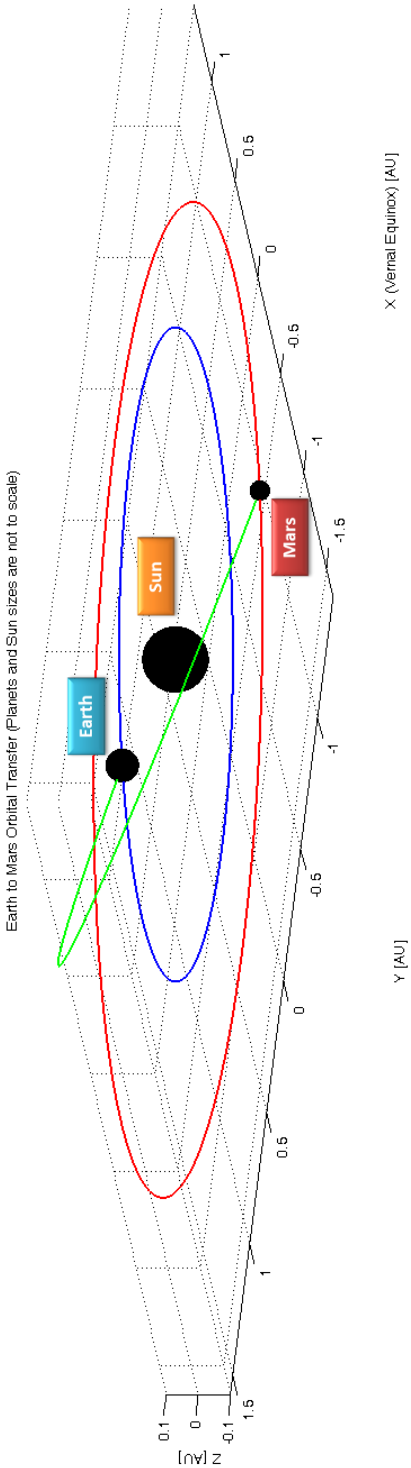

Figure 15 – An example of an Earth-Mars trajectory with relatively high inclination.

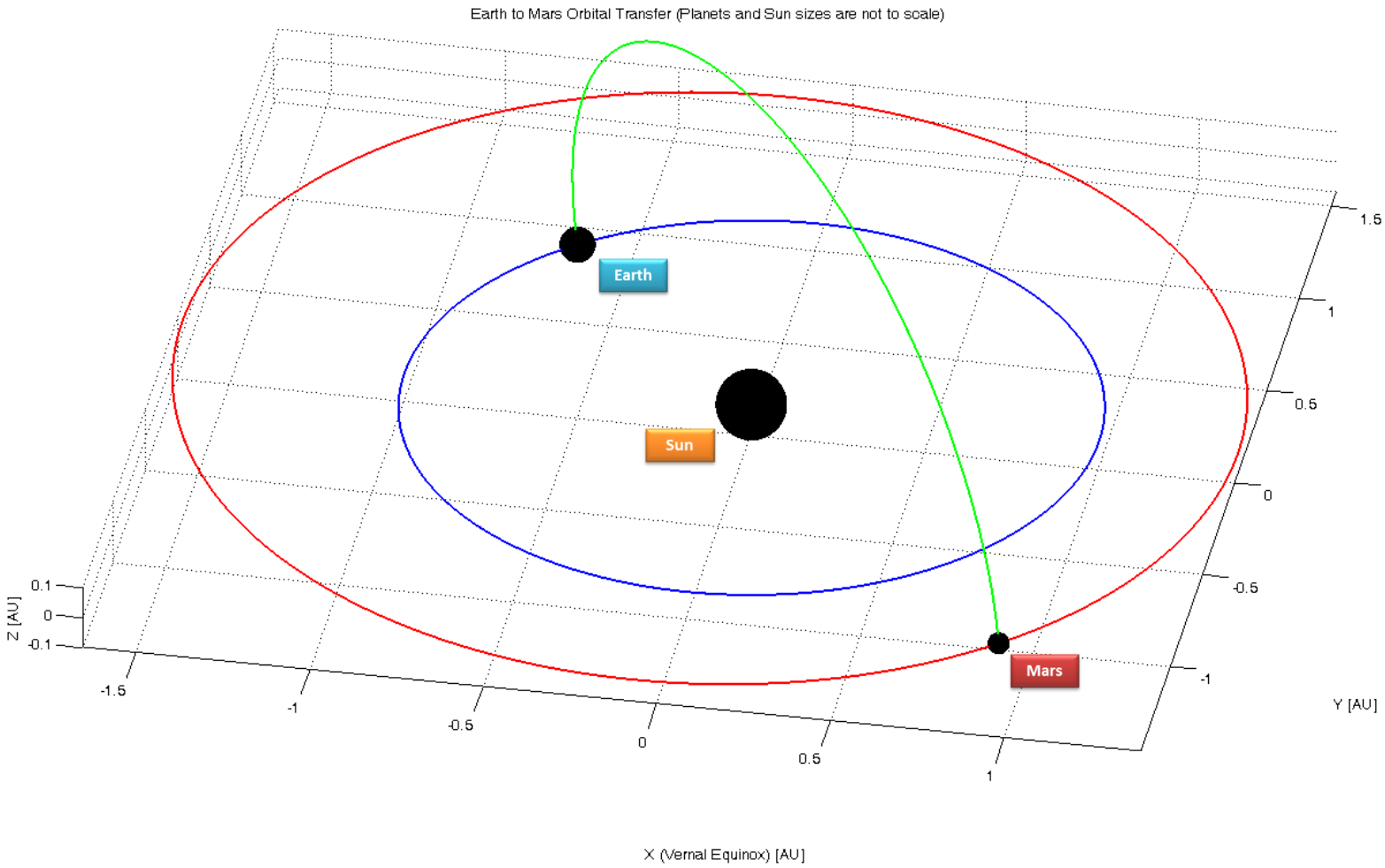

Figure 16 – Example of an extremely high inclination orbital transfer from Earth to Mars.

Trajectory Examples

This section presents the graphical representation of transfer trajectories Earth-Mars of various spacecraft that were launched in the past and that are planned to be launched in the near future. Table 4 summarizes what is presented in Figures 17 – 20.

Table 4 – Summary of trajectories presented in this section.

Earth-Mars Trajectories of Various Spacecraft			
Spacecraft Name	**Launch Date**	**Arrival Date**	**Figure #**
Mariner 4[1]	November 28, 1964	July 14, 1965	17
Mars Reconnaissance Orbiter (MRO) [2]	August 12, 2005	March 10, 2006	18
Mars Science Laboratory[3]	November 26, 2011	August 6, 2012	19
Mars Atmosphere and Volatile EvolutioN (MAVEN) [5]	November 18, 2013*	September 22, 2014*+	20

*nominal dates; +expected date of Mars orbital insertion

As Figures 17 – 20 show, spacecraft that have been launched to Mars follow trajectories that have a transfer angle $\Delta\theta$ close to $180°$. In fact, as discussed in more details in Chapter 6, analytical solutions for the case $\Delta\theta = 180°$ exist and are known as Hohmann transfers.

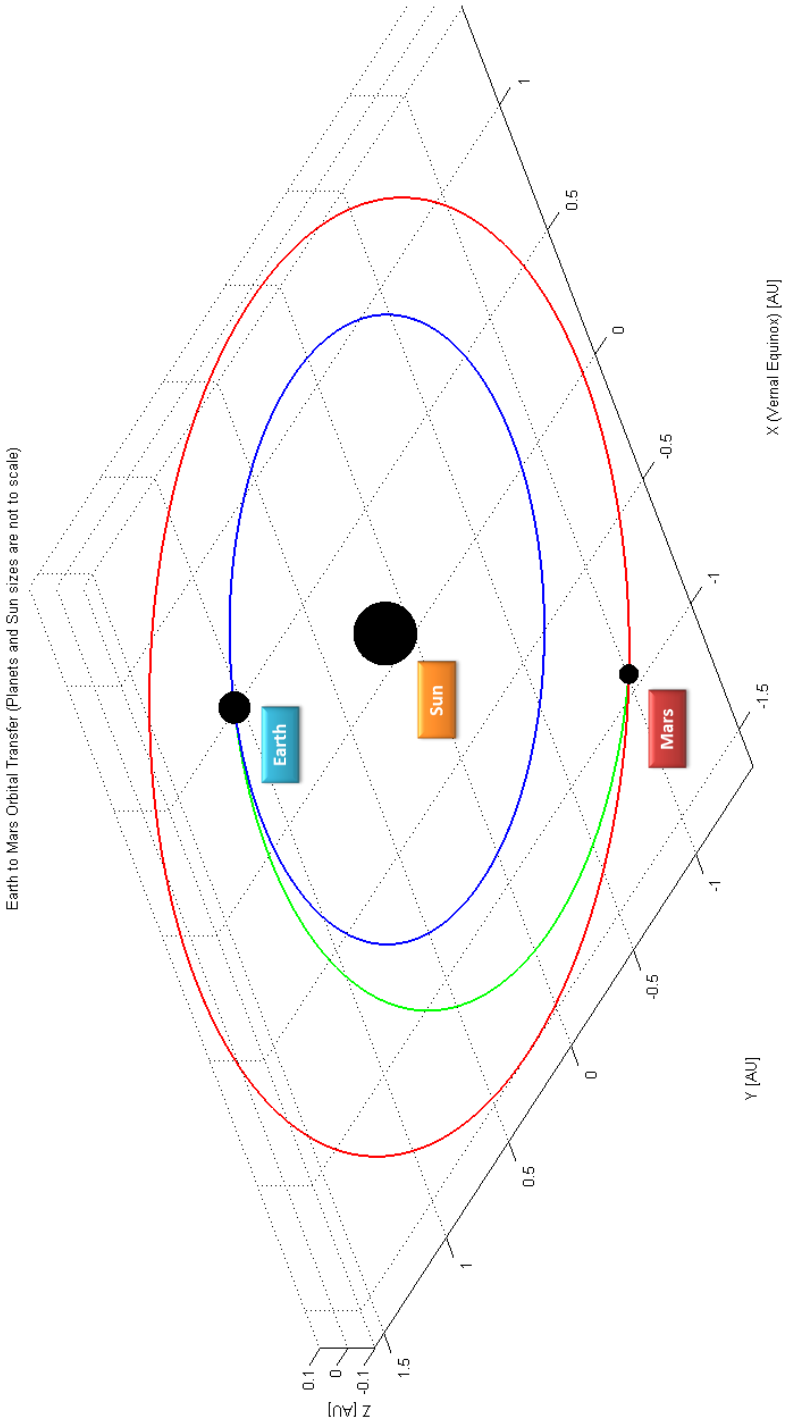

Figure 17 – Mariner 4 trajectory.

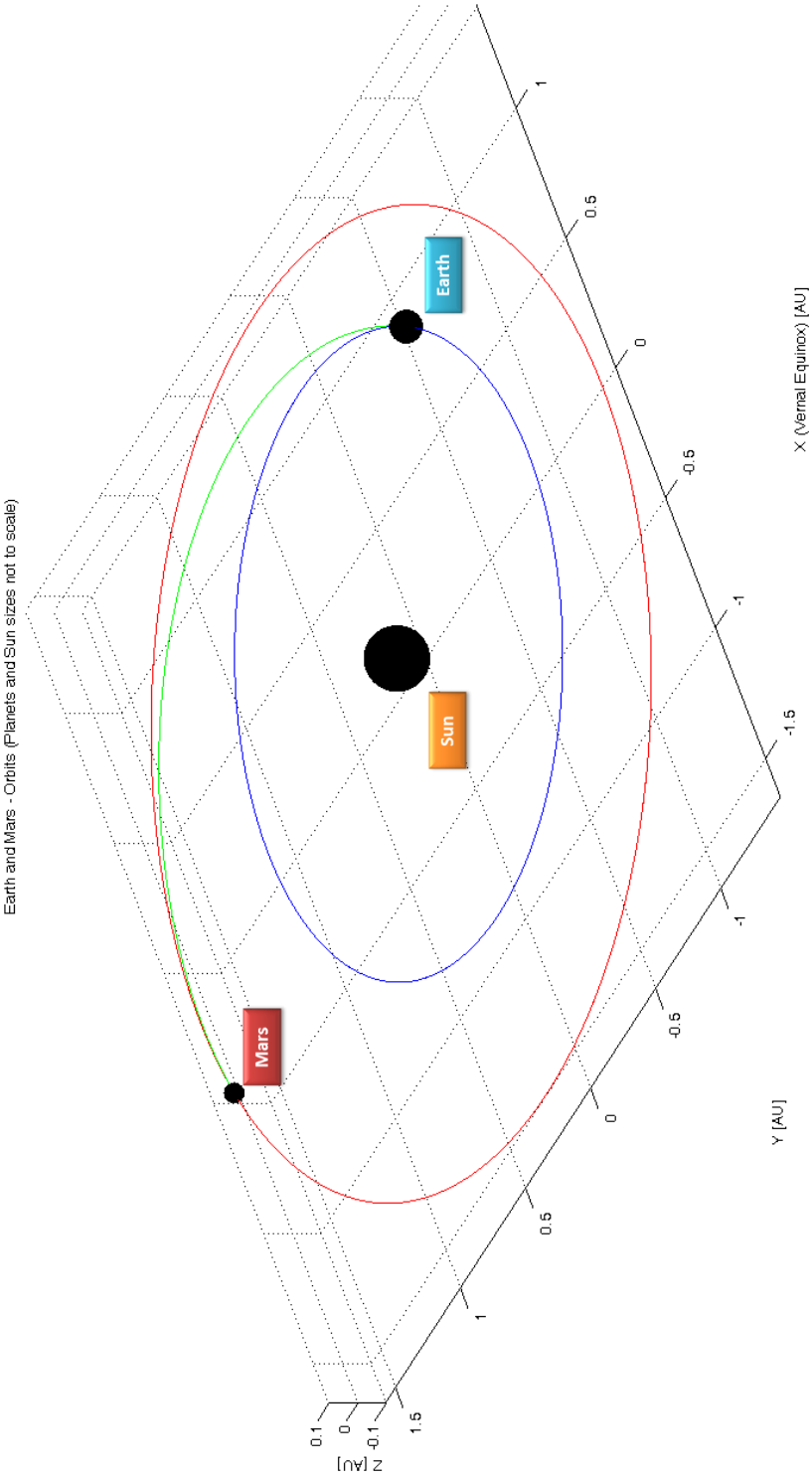

Figure 18 – MRO trajectory.

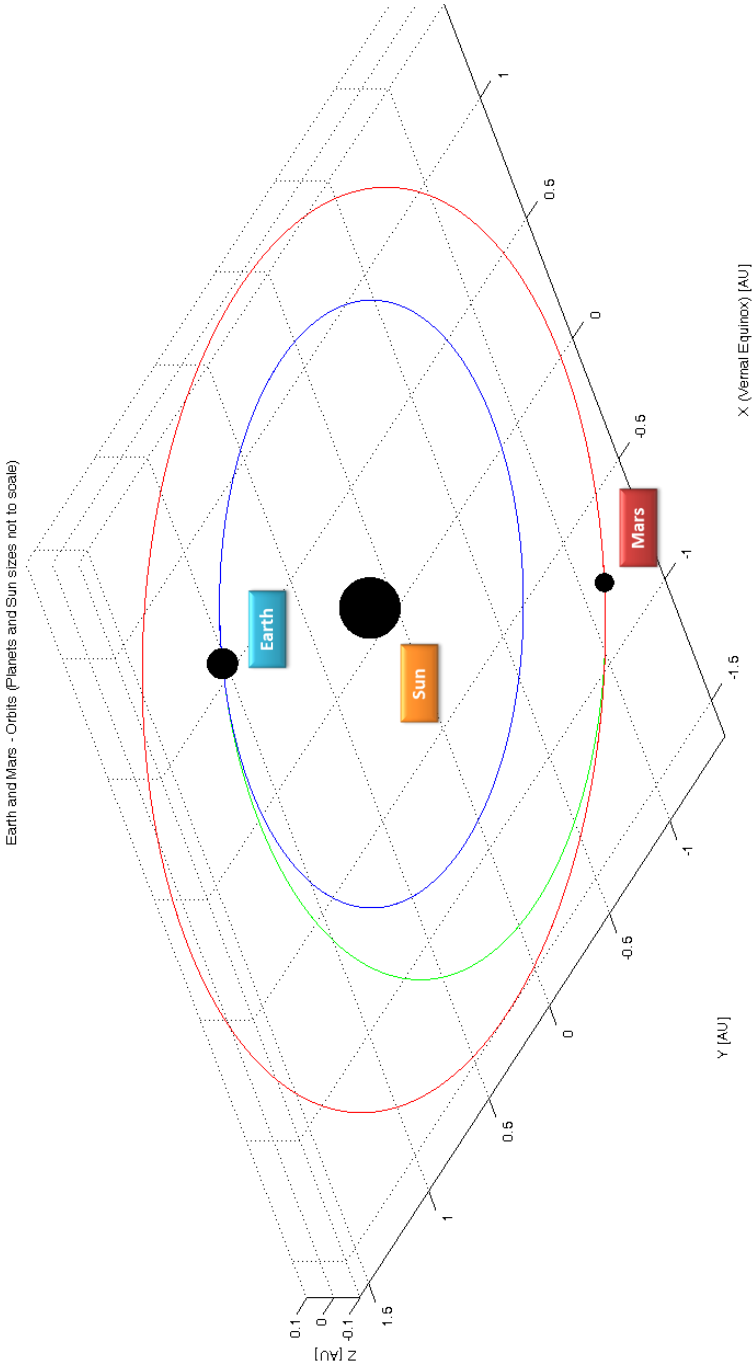

Figure 19 – Mars Science Laboratory trajectory.

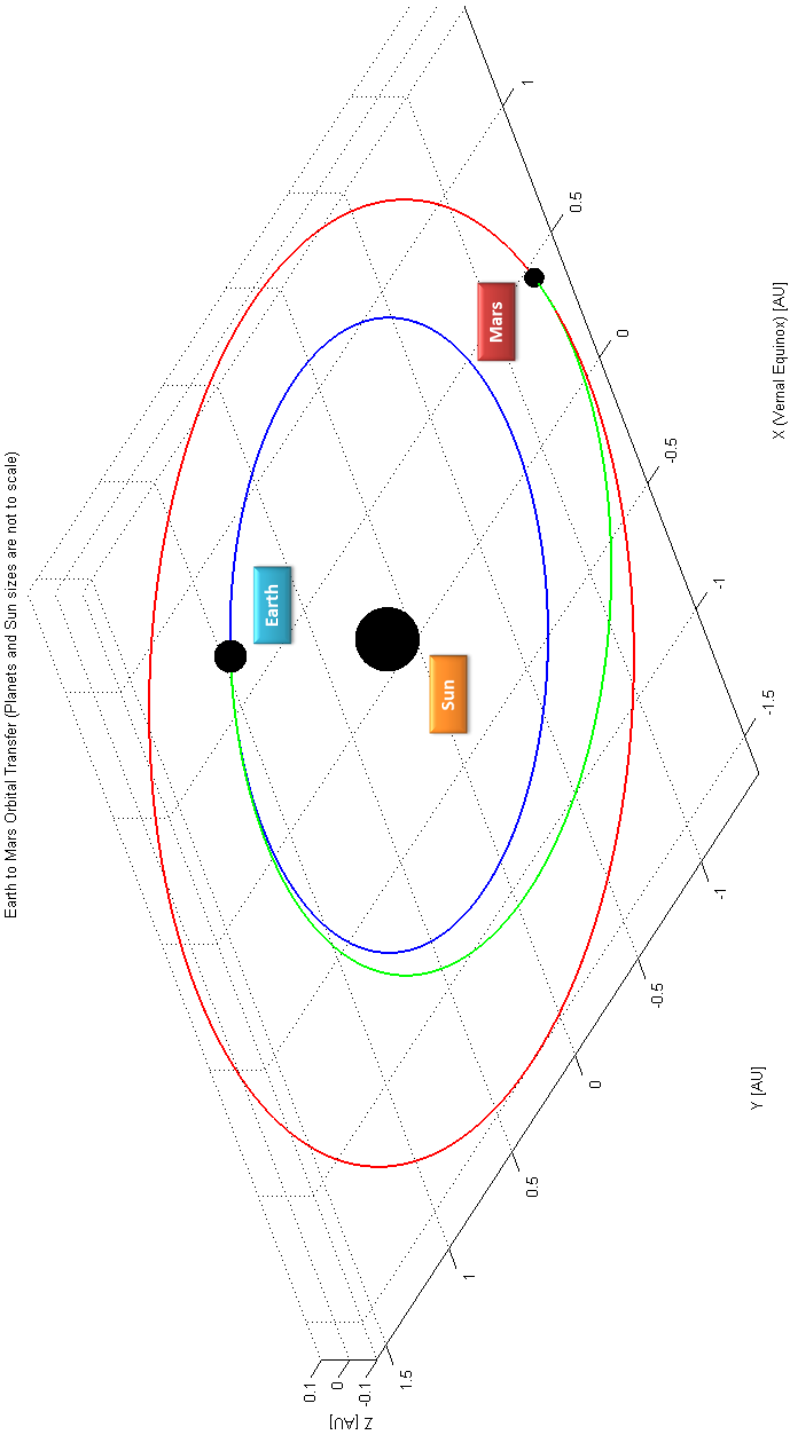

Figure 20 – MAVEN trajectory.

Extreme Cases

Sometimes it is useful to consider cases of hyperbolic transfers. In fact, as previously mentioned in the Eccentricity section, hyperbolic transfers usually provide much shorter times of flight than elliptical orbits. As opposed to elliptical cases, when $e > 1$ both $C3$ and v_∞ increase drastically as time of flight decreases. Therefore, in order to use such transfers it is necessary to have a propulsion system capable of performing extremely high Δv maneuvers in a relatively short amount of time, i.e. high thrust. Previous research, such as the NERVA project, has shown that nuclear propulsion systems would be capable of with specific impulse in the order of 900-1000 seconds, which is at least twice as much as typical chemical rockets.[11] Such a high I_{sp} would decrease the amount of propellant needed to accomplish the mission and allow for a bigger payload mass. Examples of low time of flight hyperbolic trajectories are shown in Figure 21 –24 and summarized in Table 5.

Table 5 – Summary of some examples of hyperbolic trajectories with low transfer times.

Examples of Hyperbolic Earth-Mars Trajectories				
Launch Date	**Arrival Date**	**TOF (days)**	**Eccentricity**	**Figure #**
January 1, 2029	March 1, 2029	59	2.033	21
February 1, 2031	April 1, 2031	59	1.986	22
May 1, 2033	June 15, 2033	45	1.308	23
July 1, 2035	August 1, 2053	31	2.639	24

Note that the most propellant-convenient hyperbolic trajectories with low time of flight take place close to the dates of the opposition of Earth and Mars. In fact, when two planets are in opposition their distance is minimized. On the other hand, it would be extremely inconvenient to launch a spacecraft from Earth away from the Sun towards Mars since the spacecraft propulsion system would have to directly "fight" against the Sun's gravitational force. Therefore, for the examples listed above, departure and arrival dates that are 30-45 days before and/or after the

opposition of the two planets were considered. For more details regarding the trajectories taken into account see Appendix C. Additionally, other hyperbolic trajectory cases are presented in Chapter 6.

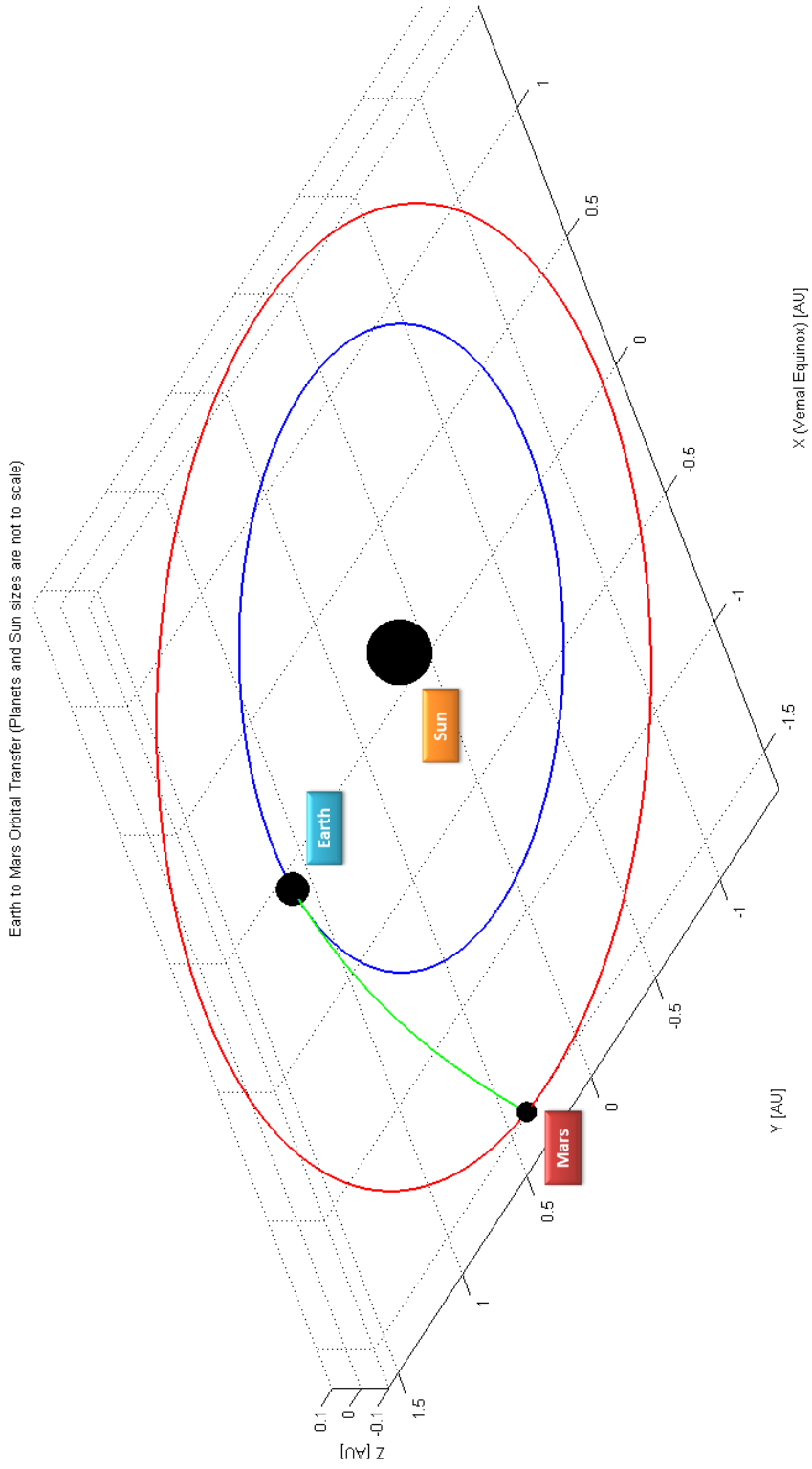

Figure 21 – Hyperbolic Earth-Mars trajectory case 1.

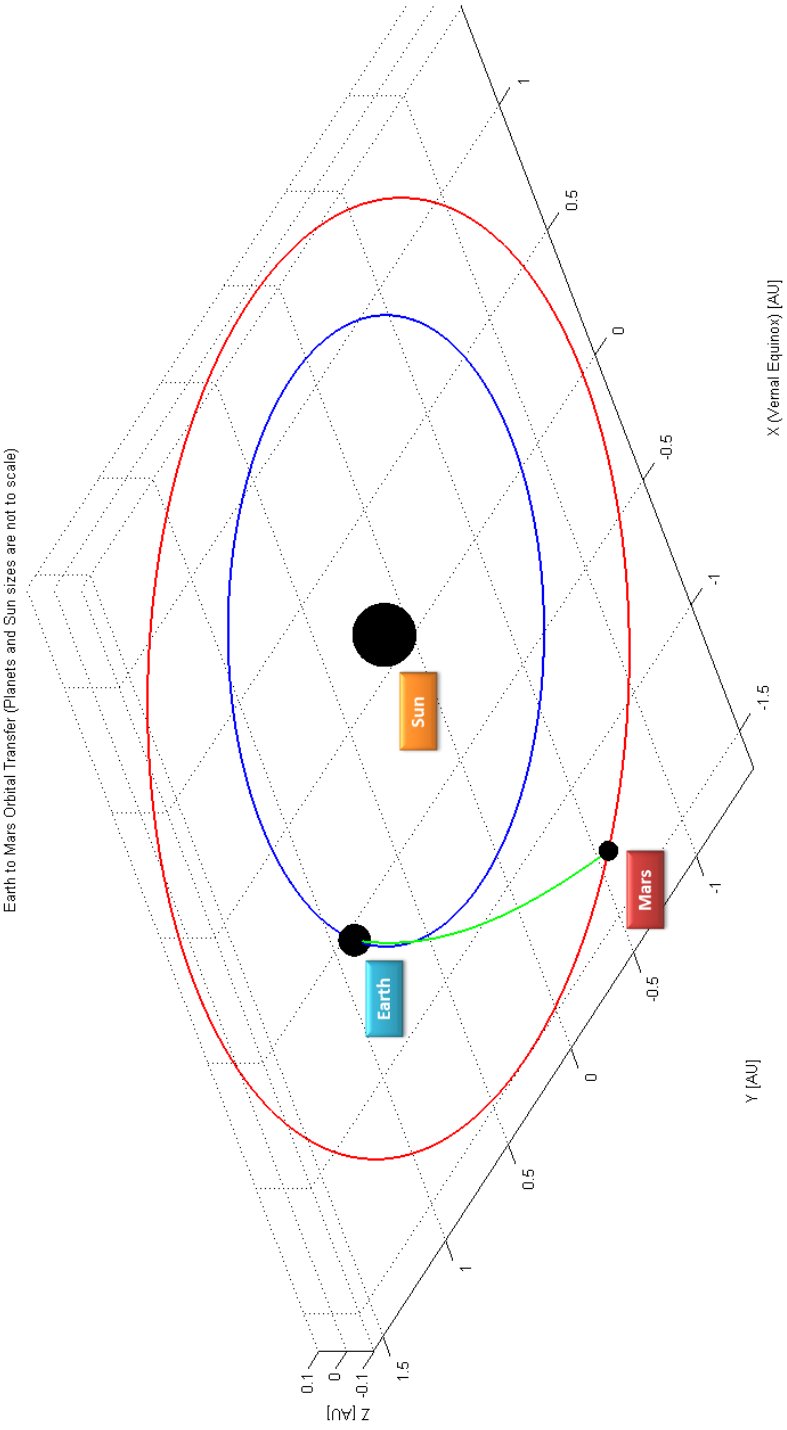

Figure 22 – Hyperbolic Earth-Mars trajectory case 2.

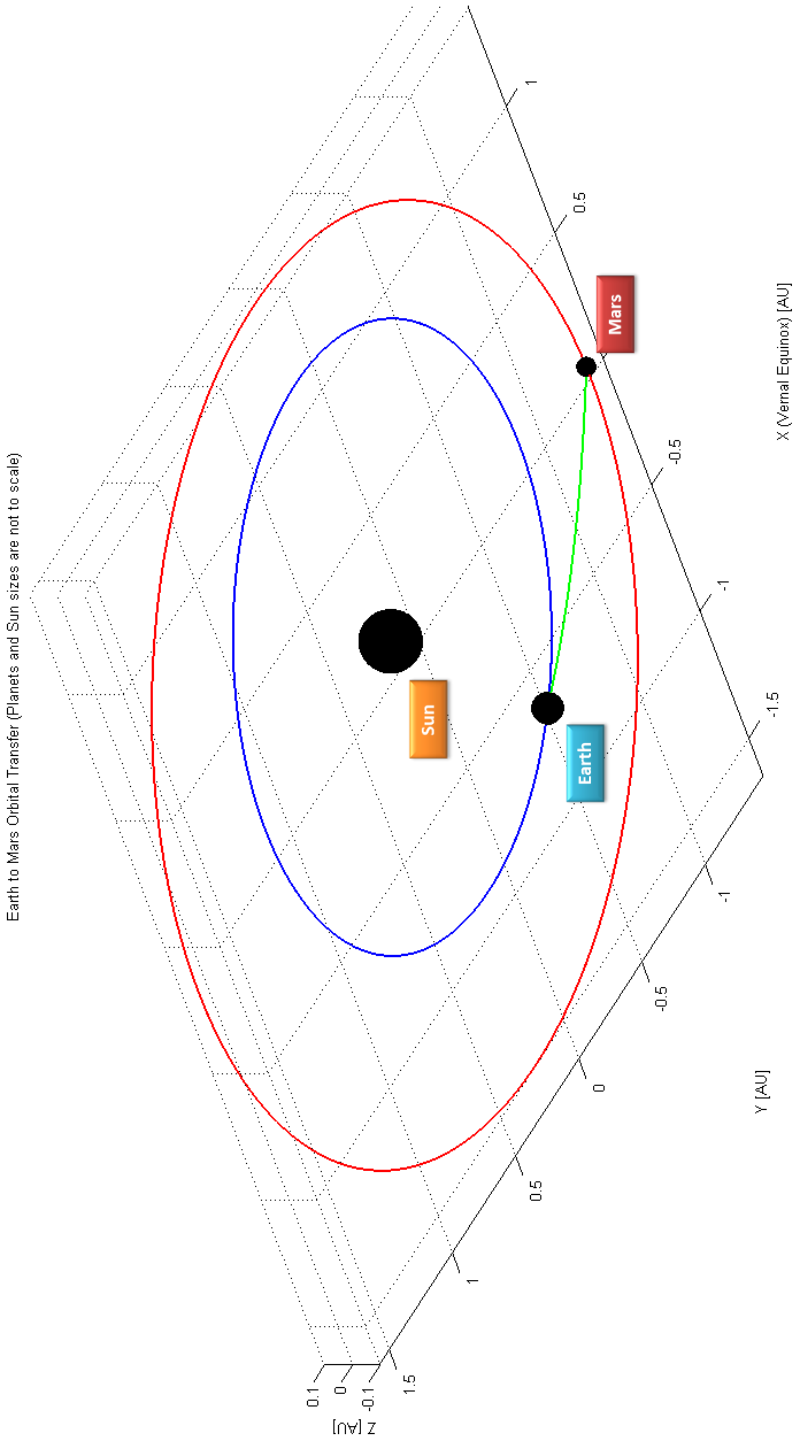

Figure 23 – Hyperbolic Earth-Mars trajectory case 3.

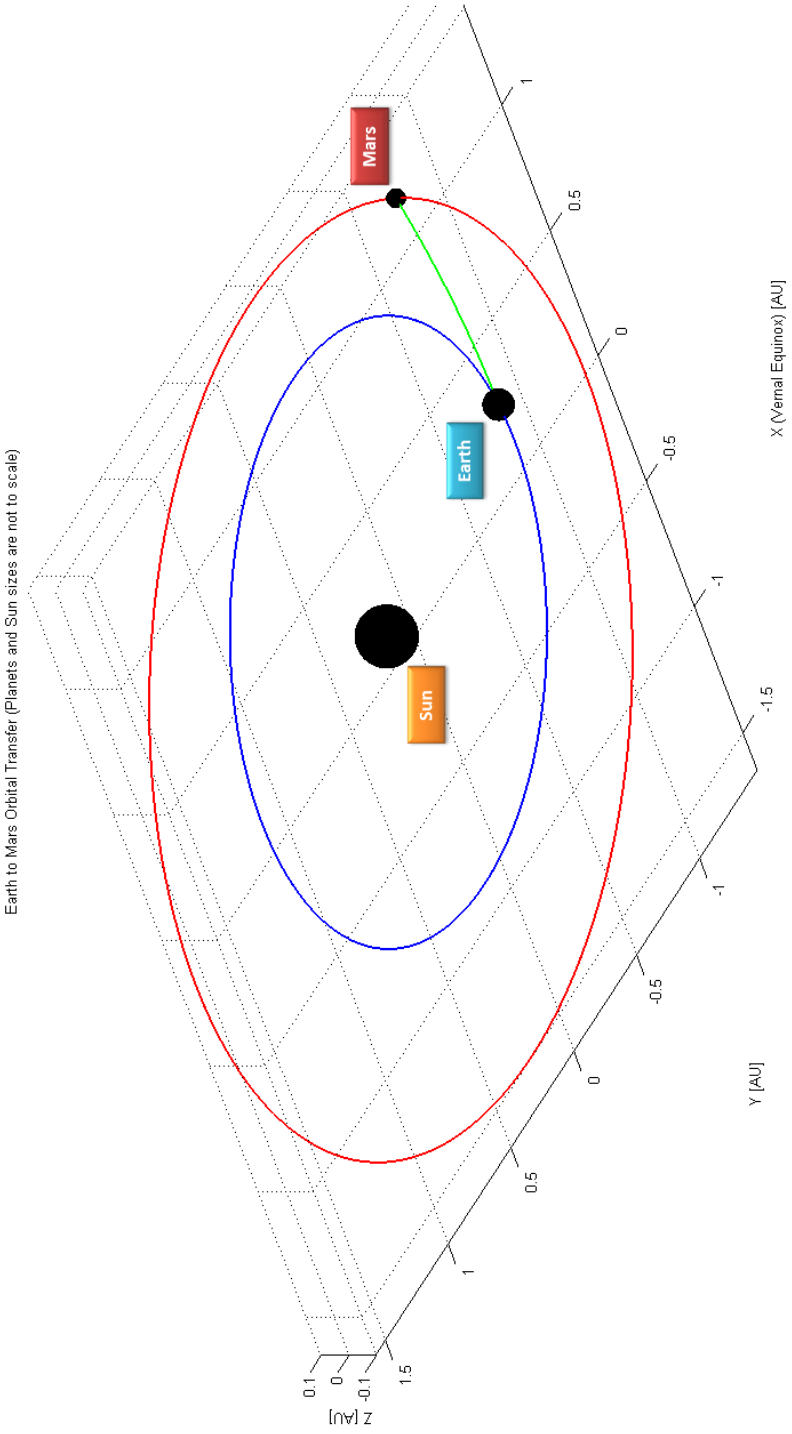

Figure 24 – Hyperbolic Earth-Mars trajectory case 4.

Chapter 6

A Particular Case and Applications

As previously discussed, the solution to Lambert's Problem does not always give reasonable results in terms of values of $C3$, v_∞ and inclination of the transfer orbit for cases close to $\Delta\theta = 0°$ or $\Delta\theta = 180°$. Making the rational assumption that Earth and Mars have coplanar circular orbits, it is possible to analyze the $\Delta\theta = 180°$ case analytically. This particular case is the classic Hohmann transfer.

The Hohmann Transfer

The case of the Hohmann transfer is particular since the transfer angle between the departure planet and arrival planet is considered to be exactly 180°. Additionally, it is well known that the Hohmann transfer is the most energy efficient two-burn maneuver for transferring between two coplanar circular orbits sharing a common focus. This makes the Hohmann transfer the most propellant efficient transfer between two planets orbiting the Sun. It also must be noted that analytical solutions to find the total Δv for Hohmann transfers exist with the additional assumption that Earth and Mars have circular and coplanar orbits. Knowing the initial (Earth) and final (Mars) orbital parameters of a desired spacecraft and the propulsion system I_{sp}, an algorithm that solves the Hohmann transfer problem can be implemented (in this case MATLAB was used). An example of input and output is summarized in Table 6. For launch opportunities and arrival dates for future Hohmann transfers refer to Table 7.

Table 6 – Example of a Hohmann transfer from Earth to Mars

Hohmann Transfer Example			
Input Parameters			
Initial Earth orbit altitude	*Final Mars orbit altitude*	*Specific Impulse*	
300 km	5982 km*	350 seconds	
Results			
Departure ΔV	*Arrival ΔV*	*TOF*	*Propellant mass %*
3.590 km/s	1.881 km/s	259 days	79.68%

*this altitude corresponds to the average distance of the Martian moon Phobos from Mars.

Although the Hohmann transfer is the most fuel efficient orbital maneuver between two circular and coplanar orbits (the total Δv is about 5.5 – 5.6 km/s), it is not considered to be a "fast transfer." In fact, while a Hohmann transfer from Earth to Mars requires a time of flight of approximately 260 days, it is possible to create faster trajectories to accomplish the same mission in much less time as discussed in Chapter 5 in the section *Extreme Cases*. Faster trajectories involving higher Δv maneuvers are discussed next.

Application of Lambert's Problem to Fast Trajectories

As previously discussed, given a propulsion system with high enough specific impulse, it would possible to utilize faster trajectories in a way that would make interplanetary manned missions to Mars possible. In fact, two of the primary limiting factors in a manned mission to Mars are mission duration and amount of propellant available to accomplish such mission. The former is a direct consequence of the biological response of the human body to interplanetary radiation and microgravity as well as the limited amount of resources, such as food and oxygen, that can be transported to sustain the crew. The latter mainly depends on the propulsion system used and the Δv maneuvers that need to be performed in order to leave Earth's sphere of

influence and to establish a closed orbit around Mars. While the development of more efficient propulsion systems is most definitely a necessity for manned missions to Mars, selecting a trajectory that would minimize both time of flight and total Δv (and hence minimize propellant mass) simultaneously is also a key decision in designing the mission.

For the following analysis, only the outbound Earth-Mars trajectory was considered. A similar analysis can be done for the return trip Mars-Earth. Furthermore, only trajectories with a time of flight lower than 150 days ($TOF_{max} = 150$) were taken into account. Additionally, only reasonable orbital transfers were considered by setting an upper bound to maximum Δv_{tot} as a function of I_{sp}

$$\Delta v_{tot,max} = g_0 I_{sp} \ln\left(\frac{1}{1-R_p}\right) \tag{53}$$

where $R_p = \left(\frac{m_p}{m_1}\right)_{max}$, i.e. the maximum propellant to total mass ratio to be considered for the mission. For this analysis, R_p was varied between 0.85 and 0.9 and I_{sp} was kept constant at a value of 1000 seconds. Note that examples of fast transfer were presented in the previous section, although they are not yet technologically feasible due to their extremely high Δv_{tot} (refer to Appendix C for additional details).

Theoretically, there are an infinite amount of possible trajectories from Earth to Mars, but only those occurring up to about two months before and two months after an Earth-Mars opposition were considered. This is due to the fact that this situation results in the shortest distances Earth-Mars. Oppositions occurring in the future are listed in Table 7.

Table 7 – Earth-Mars oppositions and launch opportunities, 2014-2036. Launch opportunities and arrival dates assume a Hohmann transfer.[15]

Launch Opportunity	Opposition	Arrival Date
12/31/13	4/7/14	9/16/14
2/15/16	5/22/16	10/31/16
4/20/18	7/26/18	1/4/19
7/8/20	10/13/20	3/24/21
9/1/22	12/7/22	5/18/23
10/10/24	1/15/25	6/26/25
11/14/26	2/19/27	7/31/27
12/18/28	3/25/29	9/3/29
1/25/31	5/2/31	10/11/31
3/22/33	6/27/33	12/6/33
6/10/35	9/15/35	4/24/36

In order to identify the most effective trajectories in terms of time of flight (TOF, in seconds) and Δv_{tot}, the following efficiency parameter is introduced

$$\eta = \frac{1}{TOF * \Delta v_{tot}} \tag{54}$$

Therefore, it is now possible to compare various orbital transfers using η. In fact, trajectories with higher values of η are preferable. Next are some examples transfers with TOF less than 150 days.

Figure 25 shows an example of a contour plot of trajectory efficiency η (in blue) around the 2029 Earth-Mars opposition. In red and green are $\Delta v_{tot,max}$ and TOF_{max} respectively; all possible admissible solutions are therefore constrained to be under the green line and above the red line (in Figure 25, only solutions to the right of the red and green line crossing are possible).

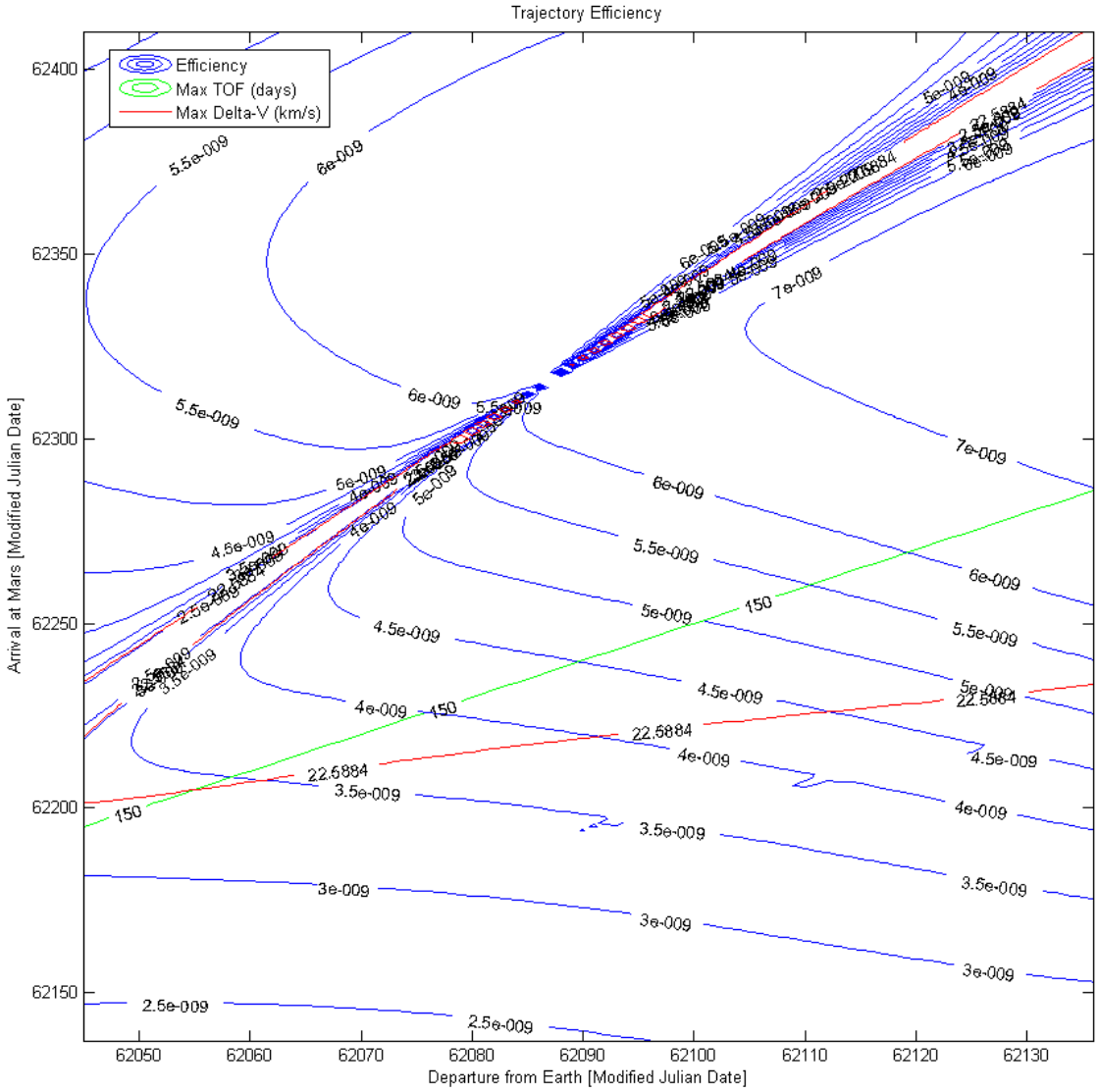

Figure 25 – Contour plot of trajectory efficiency η centered about the 2029 opposition.

Note that usually Δv_{tot} goes up as TOF goes down, hence making the maximization of η not trivial. Additionally, the regions on the graph where η is not smooth is due to the changing from $e < 1$ to $e > 1$. In fact, the solution to Lambert's problem close to $e = 1$ requires more iterations to converge and is sometimes slightly inaccurate from a numerical perspective. Two additional examples of trajectory efficiency plots are presented in Figures 26 and Figure 27.

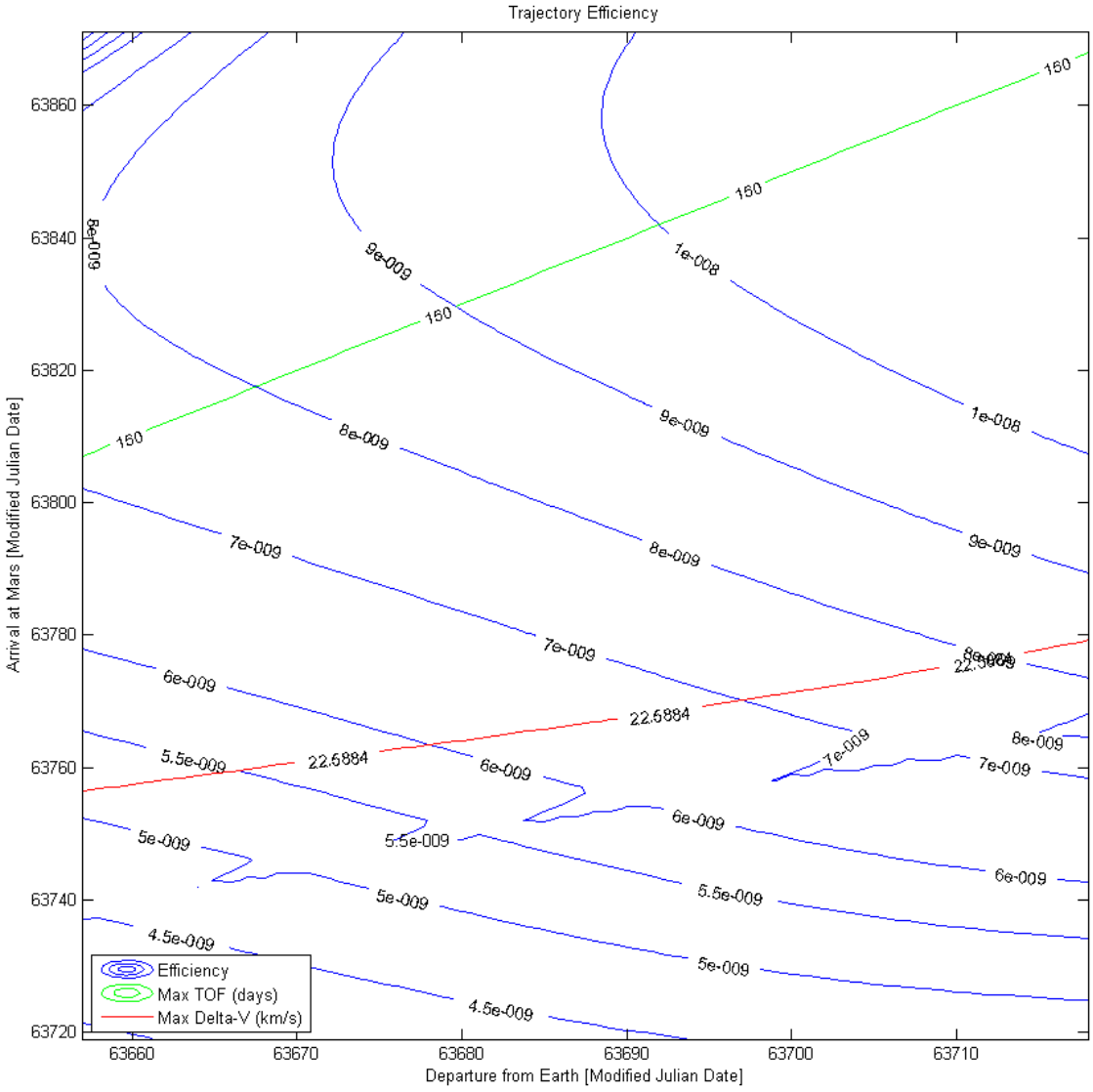

Figure 26 – Contour plot of trajectory efficiency η centered about the 2033 opposition.

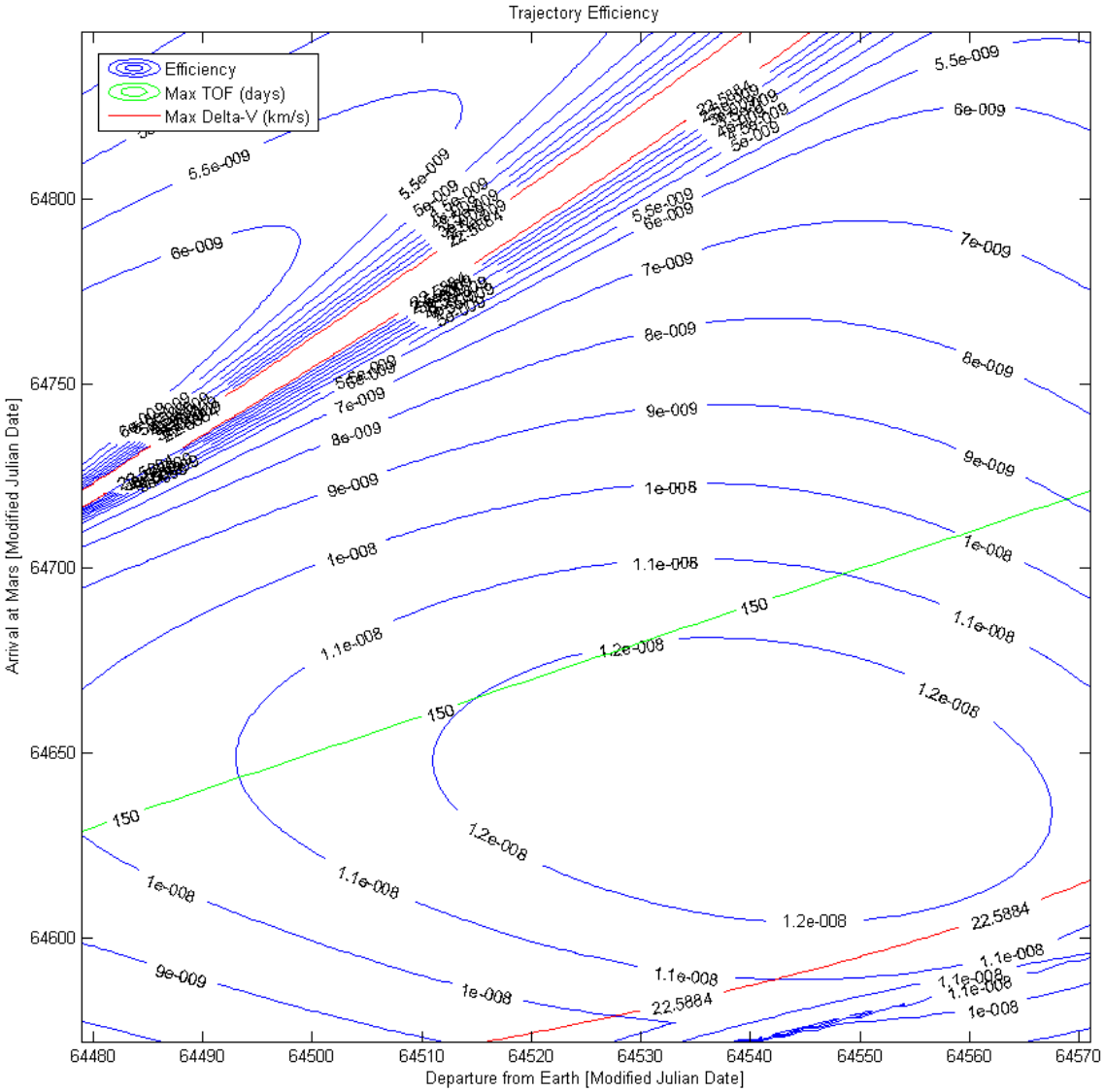

Figure 27 – Contour plot of trajectory efficiency η centered about the 2035 opposition.

Details about the solutions with the highest η for the three examples presented are summarized on Table 8. Furthermore, the trajectories of such optimized trajectories are given in Figures 28-30.

Table 8 – Earth-Mars fast transfers with highest efficiency for $TOF_{max} = 150$ days and $I_{sp} = 1000$ seconds.

Examples of Reasonable Earth-Mars Fast Transfers with $\eta = \eta_{max}$				
Launch Date	**Arrival Date**	**TOF (days)**	**Δv_{tot} (km/s)**	**Figure #**
December 31, 2028	May 20, 2029	150	11.051	28
May 1, 2033	September 15, 2033	137	7.410	29
August 3, 2035	November 10, 2035	99	9.000	30

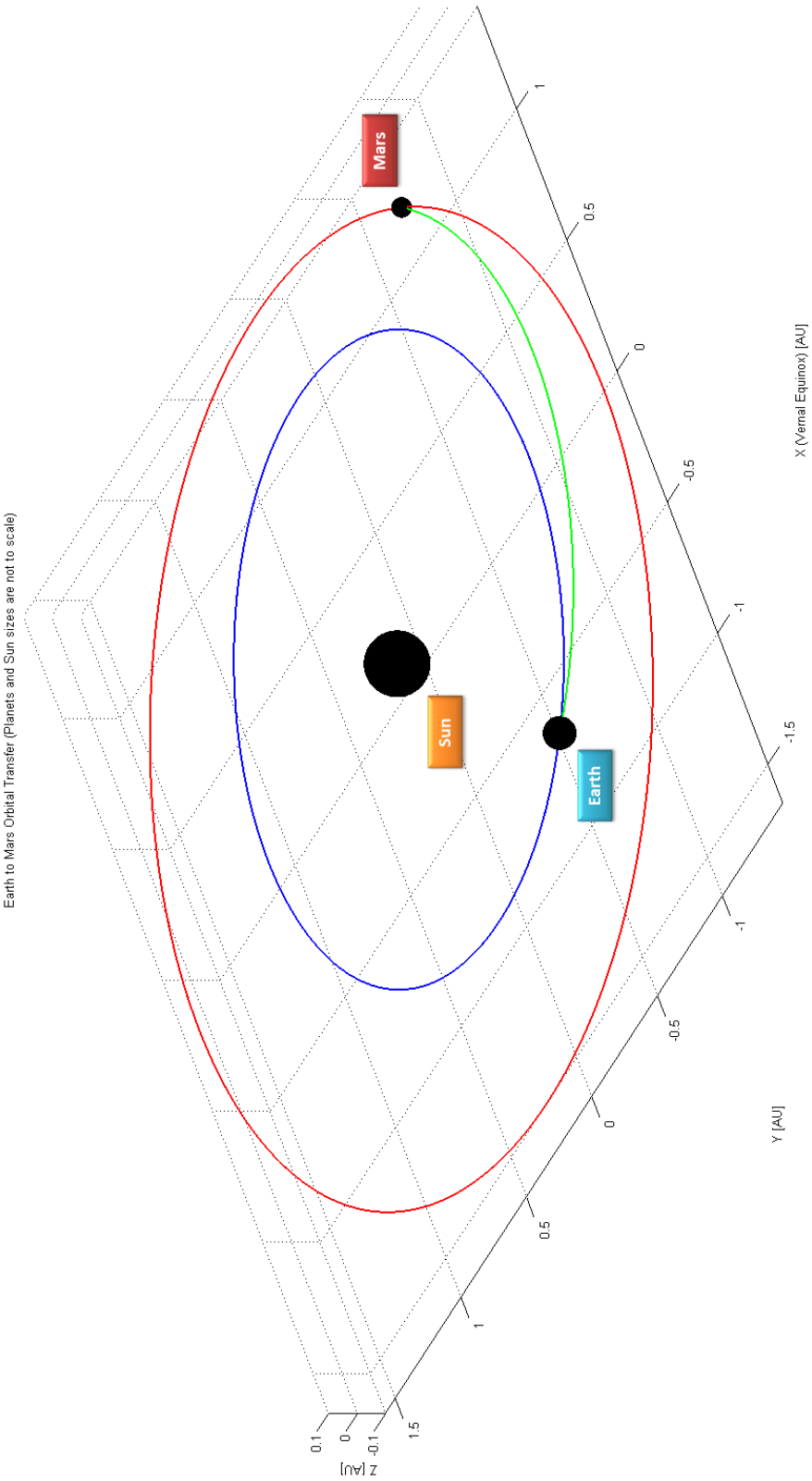

Figure 28 – Earth-Mars optimized fast transfer for the year 2028-2029.

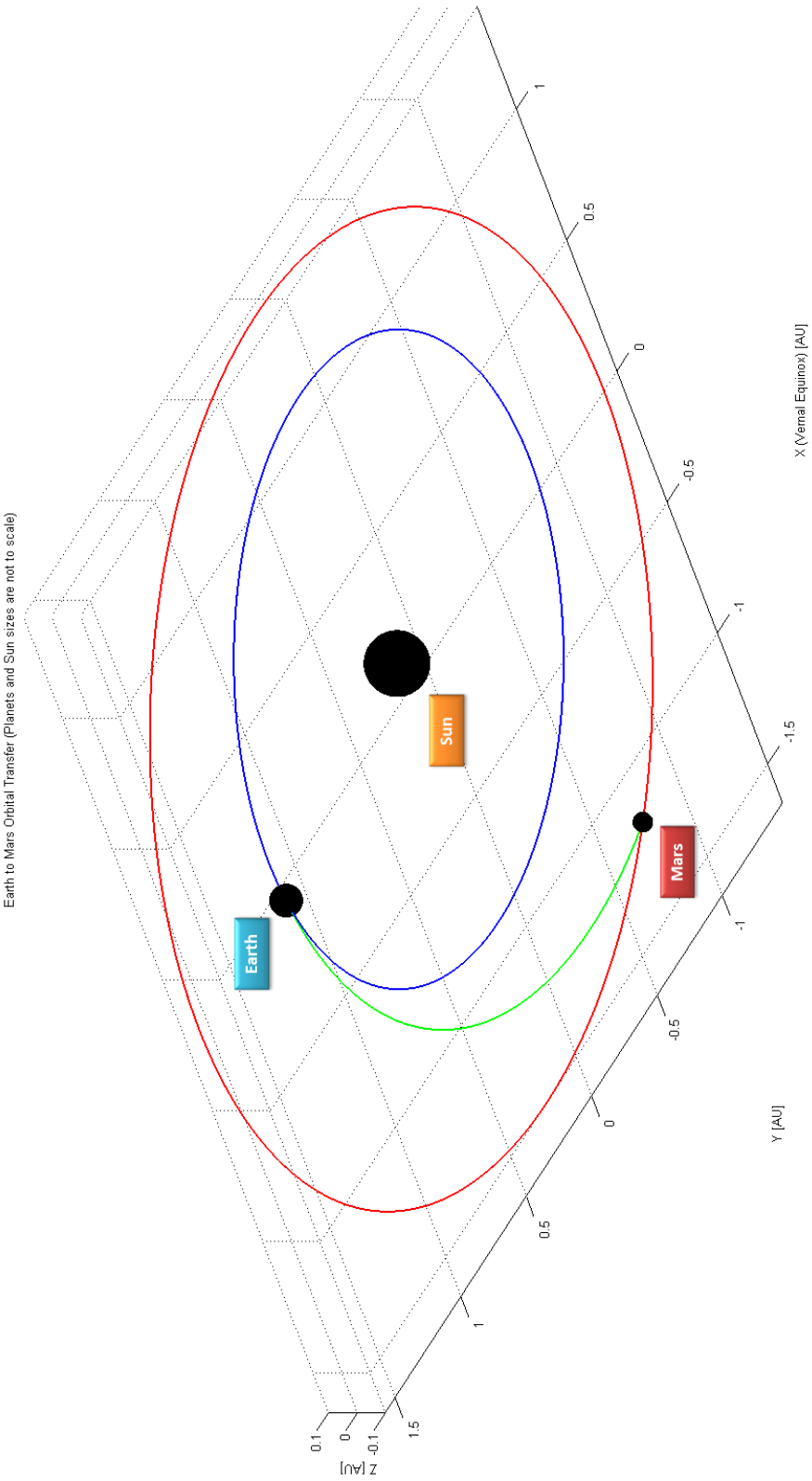

Figure 29 – Earth-Mars optimized fast transfer for the year 2033.

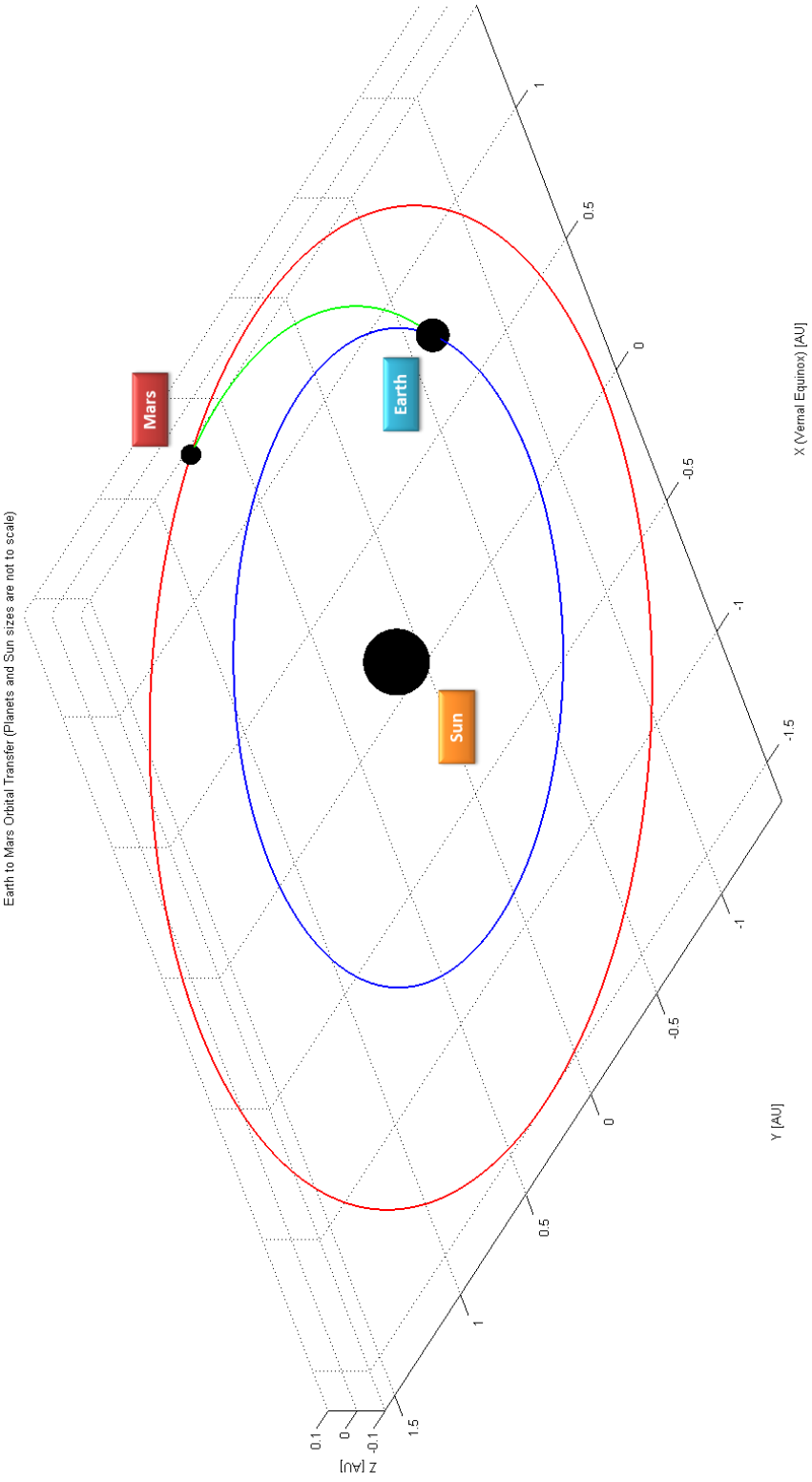

Figure 30 – Earth-Mars optimized fast transfer for the year 2035.

Conclusion and Future Work

The analyses and results presented in this thesis give an idea of the difficulties a mission from Earth to Mars can present from an astrodynamics point of view. Some of these challenges include the Δv maneuvers (and hence the amount of propellant) required to leave Earth's sphere of influence and to establish a closed orbit around Mars upon arrival and the time of flight needed for the transfer orbit to take place. This last one is especially critical when discussing human missions.

In this thesis, some important and useful tools to analyze and decide mission parameters related to the outbound Earth-Mars possible trajectories are discussed. One of these, and perhaps the most important mentioned throughout the thesis, is porkchop plots. Knowing the position and velocity vectors of the departure and arrival planets for given departure and arrival dates, it is possible to solve Lambert's problem. Many methods for solving Lambert's problem exist and the one presented in Chapter 3 makes use of the universal variable. From the solution to Lambert's problem and knowing the desired initial and final parking orbits about Earth and Mars respectively, porkchop plots can be created. Space agencies such as NASA and ESA create and utilize porkchop plots to determine the possible launch and arrival windows for various missions, including missions to Mars. In fact, given the launch vehicle and upper stage capabilities, the scientific mission requirements and the results of porkchop plots, nominal launch and arrival dates can be established.

Along with the optimal type I and type II orbital transfers (i.e. those transfers whose Δv is minimized) results from Lambert's problem can help determine the geometry of the transfer orbit. As shown in various examples of trajectories presented in Chapter 5 and Chapter 6, orbital elements such as eccentricity, inclination and semimajor axis can vary greatly. In fact, for

example, since Lambert's solution fails close to orbital transfers of 180°, trajectories with extremely high inclinations should not be considered. This can be seen from the numerical results obtained using software such as MATLAB or via visual results of the actual trajectory.

Given the current state of the art chemical propulsion systems, a manned mission to Mars would not be feasible. As discussed in Chapter 5 and Chapter 6, assuming that propulsion systems with high specific impulse, such as nuclear thermal rockets, could be used, manned missions to Mars would become possible. Based on the efficiency parameter defined in Chapter 6, trajectories which are considered optimal in terms of both transfer time and total Δv can be found. For example, for the 2035 case, the optimal trajectory has a Δv_{tot} of about 9.0 km/s, which is approximately 3.5 km/s more Δv than a Hohmann transfer, although it requires a time of flight of only 99 days as opposed to the 260 days required by the Hohmann transfer. In fact, this particular trajectory has a much higher $\Delta v/day$ ratio than a classic Hohmann transfer. Thus, while increasing the value of Δv_{tot} (still to a reasonable amount), the time of flight to Mars is drastically lowered.

It must be noted the porkchop plots and related results obtained throughout this thesis would be part of a preliminary mission design. In order to get more details about an actual trajectory for a mission to Mars, more factors, such as the type of spacecraft to consider, would have to be included. For example, landing a rover, such as Curiosity, onto the Martian surface would be a much different mission than getting an orbiter, such MRO, into a science orbit about Mars. Due to the presence of an atmosphere and the complicated EDL procedures required to arrive safely onto the Martian surface, the first manned missions towards Mars might result in the exploration of the Martian moons, Phobos and Deimos. Future work would then include B-plane targeting in order to intercept the moons of Mars and how to launch from Earth such that the arrival orbital plane in the Martian sphere of influence would be close to that of one of the moons.

Appendix A

Lambert Solution – Flowchart

The following flowchart outlines the key steps in solving the Lambert Problem.

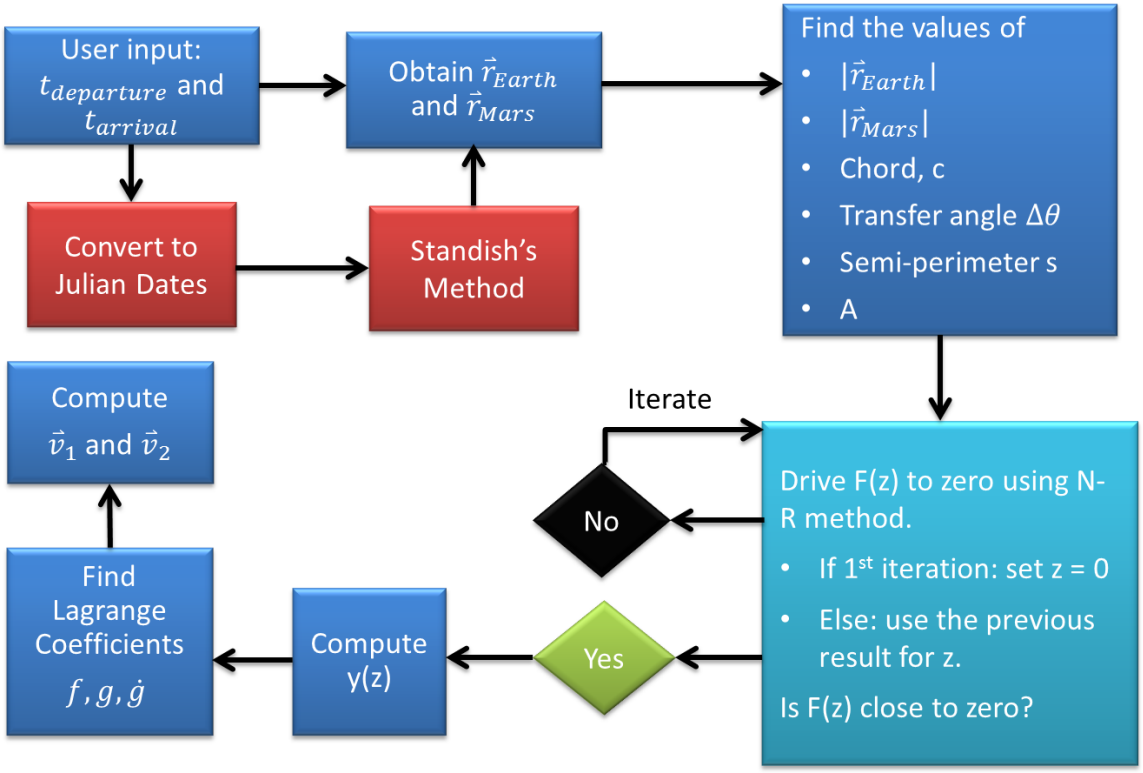

Figure A 1 – Flowchart showing the main steps when solving Lambert's problem.

Appendix B

Creating Porkchop Plots – Flowchart

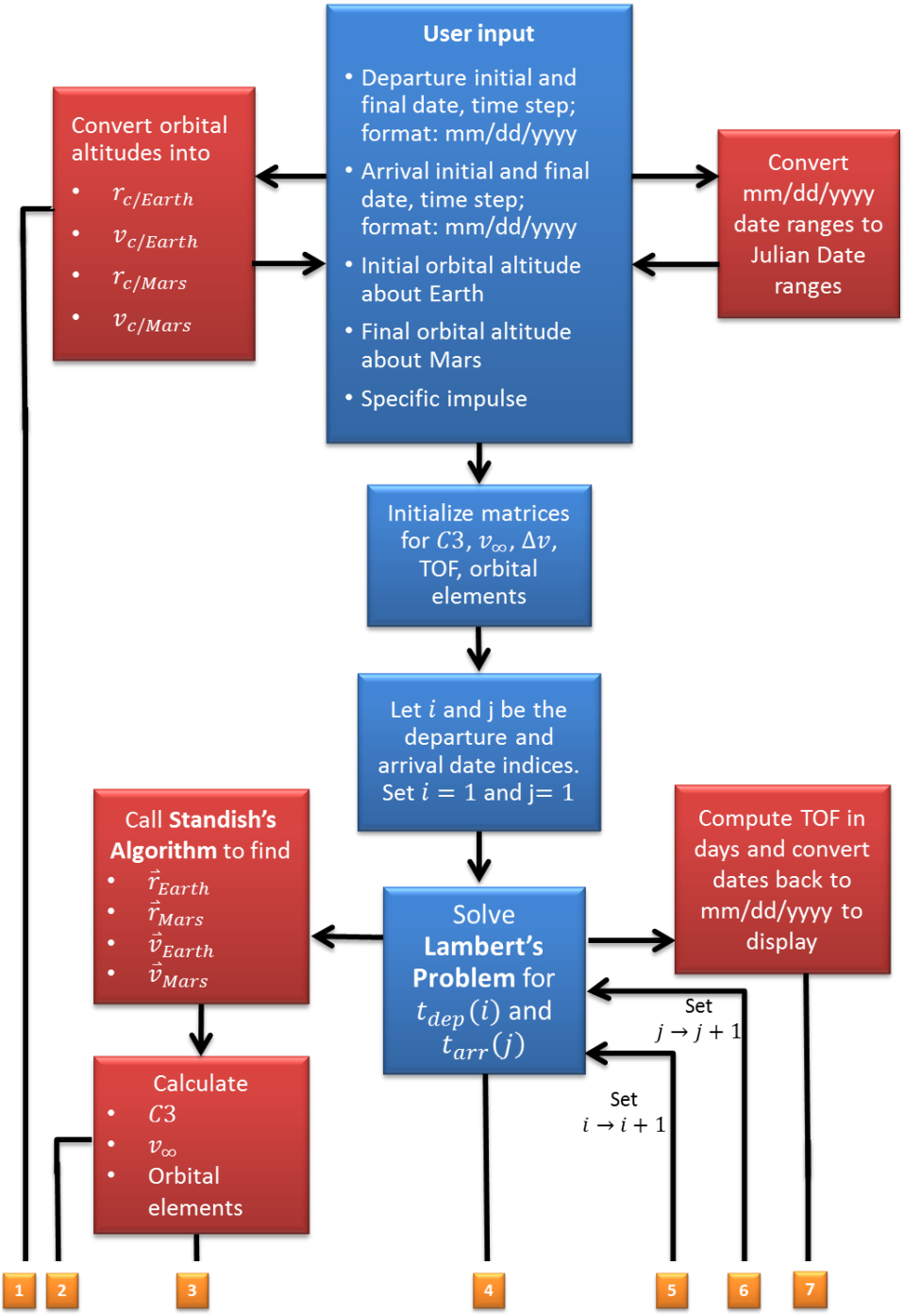

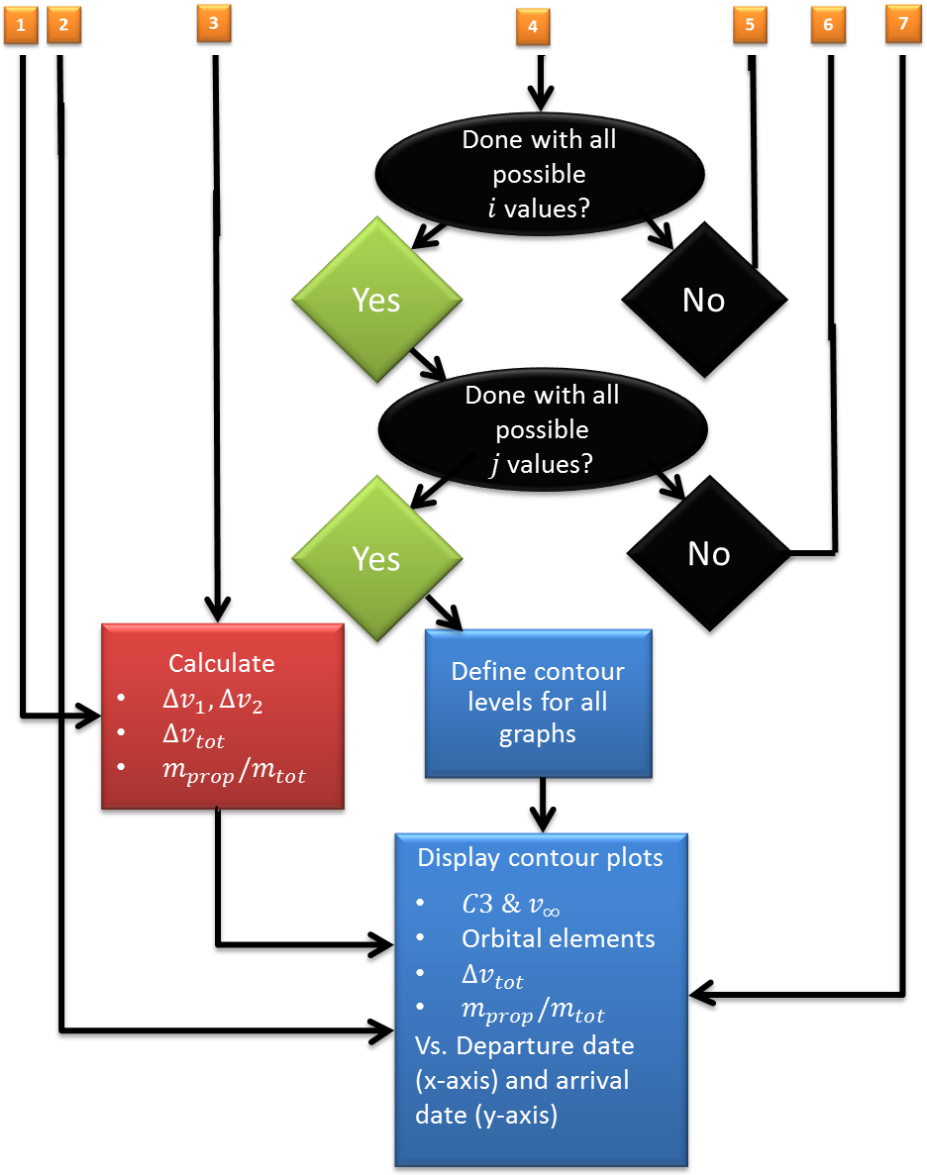

Figure B 1 – Flowchart showing the main steps when creating porkchop plots.

Appendix C

Trajectory Details

The following table presents the values of the main parameters of the various trajectories of missions conducted in the past.

Table C 1 – Earth-Mars trajectories of spacecraft sent to Mars in the past and MAVEN. All of the parameters were computed using MATLAB scripts derived from those used to compute porkchop plots.

Earth-Mars Trajectories of Various Spacecraft				
Calculated Parameters/ Spacecraft	**Mariner 4** 11/28/1964 – 7/14/1965	**MRO** 8/12/2005 – 3/10/2006	**MSL** 11/26/2011 – 8/6/2012	**MAVEN** 11/18/2013 – 9/18/2014
Launch C3 ($\boldsymbol{km^2/s^2}$)	9.85	16.33	10.68	12.08
Arrival $\boldsymbol{v_\infty}$ ($\boldsymbol{km/s}$)	4.4502	2.8384	3.5423	3.1723
Time of flight ($\boldsymbol{days}$)	228	210	254	304
Semimajor axis ($\boldsymbol{AU}$)	1.2777	1.3473	1.2607	1.2074
Eccentricity	0.228	0.248	0.219	0.199
Inclination ($\boldsymbol{degrees}$)	0.2061	3.0125	1.4952	2.0191
Argument of periapse ($\boldsymbol{degrees}$)	356.68	358.41	170.67	29.45
RAAN ($\boldsymbol{degrees}$)	65.14	-40.68	243.15	55.66
Maximum distance from the Sun	1.5548	1.6102	1.5368	1.4474

The following table presents the values of the main parameters of the various trajectories of hypothetical hyperbolic transfers for potential future missions.

Table C 2 – Earth-Mars trajectories of hypothetical future missions. All of the parameters were computed using MATLAB scripts derived from those used to compute porkchop plots.

Earth-Mars Trajectories of Hypothetical Future Missions				
Calculated Parameters/ Spacecraft	**Case 1** (1/1/2029 – 3/1/2029)	**Case 2** (2/1/2031 – 4/1/2031)	**Case 3** (5/1/2033 – 6/15/2033)	**Case 4** (7/1/2035 – 8/1/2035)
Launch C3 ($\boldsymbol{km^2/s^2}$)	496.21	495.77	273.64	748.53
Arrival $\boldsymbol{v_\infty}$ ($\boldsymbol{km/s}$)	34.2260	34.5374	26.1093	35.6000
Time of flight ($\boldsymbol{days}$)	59	59	45	31
Semimajor axis ($\boldsymbol{AU}$)	-0.9478	-0.9894	-3.1931	-0.6176
Eccentricity	2.033	1.986	1.308	2.639
Inclination ($\boldsymbol{degrees}$)	1.5952	0.7205	1.5695	2.6220
Argument of periapse ($\boldsymbol{degrees}$)	6.09	9.78	163.34	173.66
RAAN ($\boldsymbol{degrees}$)	100.58	131.72	40.59	98.65
Maximum distance from the Sun	1.6420	1.5998	1.4561	1.3831

In order to produce the results shown in this appendix, various MATLAB scripts based on the flowchart presented in Appendix B were used.

BIBLIOGRAPHY

1. "Mariner 3 & 4." *Mars Exploration Program*. NASA JPL, n.d. Web. 10 Oct. 2013. <http://mars.jpl.nasa.gov/programmissions/missions/past/mariner34/>.
2. "Mars Reconnaissance Orbiter." *Mars Reconnaissance Orbiter*. NASA JPL, n.d. Web. 10 Oct. 2013. <http://mars.jpl.nasa.gov/mro/>.
3. "Mars Science Laboratory." *Mars Science Laboratory*. NASA JPL, n.d. Web. 10 Oct. 2013. <http://mars.jpl.nasa.gov/msl/>.
4. "MATLAB." *MATLAB - The Language of Technical Computing*. MathWorks, n.d. Web. 10 Sept. 2013. <http://www.mathworks.com/products/matlab/>.
5. "MAVEN." *Mars Exploration Program*. NASA JPL, n.d. Web. 10 Oct. 2013. <http://mars.jpl.nasa.gov/programmissions/missions/future/maven/>.
6. "NASA's Mars Exploration Program." *Mars Exploration: Features*. NASA JPL, n.d. Web. 10 Nov. 2013. <http://mars.jpl.nasa.gov/spotlight/porkchopAll.html>.
7. Curtis, Howard D. *Orbital Mechanics for Engineering Students*, 2nd edition. Elsevier Aerospace Engineering Series, 2010.
8. Davis, Phil. "Solar System Exploration: Missions: In Flight." Solar System Exploration: Missions: In Flight. NASA, n.d. Web. 7 Aug. 2013. <http://solarsystem.nasa.gov/missions/profile.cfm?InFlight=1>.
9. Kemble, Stephen. *Interplanetary Mission Analysis and Design*. Berlin: Springer in Association with Praxis, 2006. Print.
10. Prussing, John E., and Bruce A. Conway. *Orbital Mechanics*. New York: Oxford UP, 1993. Print.

11. Robbins, W.H. and Finger, H.B., "An Historical Perspective of the NERVA Nuclear Rocket Engine Technology Program", NASA Contractor Report 187154/AIAA-91-3451, NASA Lewis Research Center, NASA, July 1991.
12. Standish, Erland M. Keplerian Elements for Approximate Position of the Major Planets. N.p.: NASA JPL, 2006. Print.
13. Vallado, David A. *Fundamentals of Astrodynamics and Applications*. 3rd ed. Dordrecht: Kluwer Academic, 2007. Print.
14. Yeomans, Donald K. "Keplerian Elements for Approximate Positions of the Major Planets."Keplerian Elements for Approximate Positions of the Major Planets. NASA JPL, n.d. Web. 09 Aug. 2013. <http://ssd.jpl.nasa.gov/?planet_pos>.
15. Wertz, James R., David F. Everett, and Jeffery Puschell. *Space Mission Engineering: The New SMAD.* Page 207 Microcosm Press and Springer, 2011.

ACADEMIC VITA

Davide Conte
dxc5120@psu.edu

Via Laviosa 12/19
Genova Pegli, 16156
Italy

Education

The Pennsylvania State University, University Park, PA 16802 2009 – 2014

Schreyer Honors College, Integrated Undergraduate/Graduate (IUG) Candidate

- M.S. in Aerospace Engineering 2013 – 2014
- B.S. in Aerospace Engineering 2009 – 2014
- B.S. in Mathematics 2009 – 2014

Honors and Awards

- Participated in RASC-AL 2013 (sponsored by NASA, NIA, and Boeing) as team leader of Martian Lion
  - Presented an innovative mission design for future human exploration of Mars through a written report, a presentation, and a poster session; conducted outreach events in local middle schools and Boy Scout troops to motivate young students to get involved in STEM fields with a focus on space exploration
- Space Systems Engineering Certificate (SPSYS)
- First place winner, College of Engineering Research Symposium poster competition
- Dean's List recognition every semester since Fall 2009
- Ju-jitsu black belt (Shodan), certified experienced instructor and referee
- Annually take part into the Dante Prize sponsored by the Dante Society of America
- Scholarships received in Italy: 3 from private institutions and 9 from Government (tot. of about $ 14,000)
- GeoEye Foundation Scholarship for the academic year 2012 – 2013
- Donald G. and Jayne L. Steva Scholarship for the academic year 2013 – 2014

Association Memberships/Activities

- Sigma Gamma Tau – Penn State Aerospace Honors Society member
- Penn State Astronomy Club – Secretary (2010 – 2013): manage club affairs and take notes at meetings
- Group Leader and Mentor for Schreyer Honors College Orientation 2011 and 2012:
  - Lead groups of incoming first-year students through various orientation activities

Professional Experience

- Teaching Intern (TI) for Astronautics (AERSP 309) Fall 2012
  - Worked with a faculty member (Dr. Melton) for about 10 hours per week grading, meeting students during office hours, conducting help and review sessions, writing homework and exam questions, and giving short lectures
- Mathematics and Language Tutor for Penn State Learning Fall 2010 – Present
- Learning Assistant for the PSU Dept. of Mathematics Spring 2011 – Present

Research Interest

Currently working with research advisor (Dr. Spencer) on the determination of the optimal interplanetary trajectory of an arbitrary spacecraft in order to correctly target the moons of Mars. This research includes:

- Interplanetary transfer maneuvers from Earth to Mars and determination of the orbital parameters of the transfer orbits and the relative required ΔV's and times of flights
- Orbit determination of the moons of Mars in order to land/rendezvous with them

Additionally, I am interested in continuing my studies on astrodynamics at the PhD level.

Relevant Design Work

Honors Flight Vehicle Design and Fabrication (Lecture and Laboratory)

- Worked on the design and fabrication of the PSU Zephyrus, a full-scale, 22.5-meter wing span Human Powered Aircraft (HPA) designed to compete in the Kremer Prize Competition

- Successfully flight tested the aircraft
- Worked in teams for the design, fabrication, and integration of parts of the aircraft including: wing, fuselage, propulsion system, connections
- Worked with composite materials such as carbon fiber and fiber glass
- Have taken this multi-semester course for about 4 years building a deep understanding of systems engineering, hands-on experience, and creativity in problem solving

Spacecraft Mission Design (2 courses, and participation in RASC-AL 2013):

- Worked on a team-based mission proposal for a Human-Focused Mars Mission for the 2013 Revolutionary Aerospace Systems Concepts Academic Linkage (RASC-AL) competition sponsored by NASA; the team participated to the RASC-AL 2013 Competition
- Team leader of a group of seven aerospace engineering students (team Martian Lion) with a focus on the Guidance, Navigation, and Control (GNC) subsystem